Article:
Farfan-Rios, W., Saatchi, S., Oliveras, I. et al. (15 more authors) (Accepted: 2025) Wood density variation across an Andes-to-Amazon elevational gradient. Journal of Ecology. ISSN 0022-0477 (In Press)

Wood density variation across an Andes-to-Amazon elevational gradient

William Farfan-Rios[1,2], Sassan Saatchi[3], Imma Oliveras[4,5], Yadvinder Malhi[5], Chelsea M. Robinson[6], Oliver L. Phillips[7], Alex Nina-Quispe[8], Juan A. Gibaja[9], Israel Cuba[9], Karina Garcia-Cabrera[9], Norma Salinas-Revilla[8], John Terborgh[10], Nigel Pitman[11], Rodolfo Vasquez[12], Abel Monteagudo Mendoza[12], Percy Nunez Vargas[3], Craig A. Layman[1,2], Miles R. Silman[1,2]

Affiliations

1 Andrew Sabin Center for Environment and Sustainability, and Department of Biology, Wake Forest University, Winston-Salem, NC 27109, USA

2 Herbario Vargaz (CUZ), Escuela Profesional de Biología, Universidad Nacional de San Antonio Abad del Cusco, Cusco, Peru

3 Jet Propulsion Laboratory, California Institute of Technology, Pasadena, CA 91109, USA

4 Institut de Recherche pour le Developpement Delegation Regionale Occitanie, AMAP Montpellier, FR 34398

5 Environmental Change Institute, School of Geography and the Environment, Oxford University, South Parks Road, Oxford, OX1 3QY, UK

6 Department of Geography, University of California, Los Angeles, CA 90095, USA

7 School of Geography, University of Leeds, LS2 9JT, UK

8 Pontificia Universidad Católica del Perú, Av. Universitaria 1801, Lima, Perú

9 Universidad Nacional de San Antonio Abad del Cusco, Cusco, Peru

10 Nicholas School of the Environment, Duke University, Durham, USA

11 Science and Education, The Field Museum, 1400 S. Lake Shore Drive, Chicago, IL, 60605-2496, USA

12 Jardín Botánico de Missouri, Oxapampa, Pasco, Perú

Correspondence: William Farfan-Rios (wfarfan@gmail.com)

Funding information

US National Science Foundation (NSF) Grant Number: DEB 0743666 and NSF Long-Term Research in Environmental Biology (LTREB) Grant Number: 1754647. National Aeronautics and Space Administration (NASA) Terrestrial Ecology Program Grant Number: NNH08ZDA001N-TE/ 08-TE08-0037. European Research Council (ERC) Advanced Grant Number: 291585. Natural Environment Research Council Grant Number: NE/F005806/, NE/D005590/1, and NE/N012542/1.

Acknowledgments

This paper is a product of the Andes Biodiversity and Ecosystem Research Group (ABERG; http://www.andesconservation.org/) with contributions from affiliated networks RAINFOR, GEM, and the ForestPlots.net data management utility for permanent plots. Data included in this study is the result of an extraordinary effort by a large team in Peru, including from the Universidad Nacional de San Antonio Abad de Cusco. Special thanks go to Luis Imunda and

Erickson Urquiaga for their assistance in the field sampling campaigns. SERFOR, SERNANP, and personnel of Manu National Park Peru assisted with logistics and permission to work in the protected area. Pantiacolla Tours and the Amazon Conservation Association provided logistical support. Support came from the Gordon and Betty Moore Foundation's Andes to Amazon initiative and the US National Science Foundation (NSF) DEB 0743666 and NSF Long-Term Research in Environmental Biology (LTREB) 1754647. The research in this study was also supported by the National Aeronautics and Space Administration (NASA) Terrestrial Ecology Program grant # NNH08ZDA001N-TE/ 08-TE08-0037. Support for RAINFOR and ForestPlots.net plot monitoring in Peru has come from a European Research Council (ERC) Advanced Grant (T-FORCES, "Tropical Forests in the Changing Earth System," 291585), Natural Environment Research Council grants (including NE/F005806/), NE/D005590/1, and NE/N012542/1), and the Gordon and Betty Moore Foundation.

Conflict of interest statement:

We declare that there are no conflicts of interest.

Author contributions:

William Farfan-Rios collected and analyzed the data and drafted the manuscript. Miles R. Silman collected the data and drafted the manuscript. Sassan Saatchi, Imma Oliveras, Yadvinder Malhi, Chelsea M. Robinson, Oliver L. Phillips, Alex Nina-Quispe, Juan A. Gibaja, Israel Cuba, Karina Garcia-Cabrera, Norma Salinas-Revilla, John Terborgh, Nigel Pitman, Rodolfo Vasquez, Abel Monteagudo Mendoza, Percy Nunez Vargas, Fernando Cornejo, collected the data. Craig A. Layman reviewed and edited the manuscript. All authors edited and approved the manuscript.

Statement of inclusion:

Our study brings together scientists from different countries, including authors from Peru, where the study was carried out. Local authors were instrumental from the start of the study in collecting the field data to editing the manuscript. We also work closely with the National Service of Natural Areas Protected by the State (SERNAP-Manu), with whom we share our results to contribute to managing the Manu National Park.

Data availability statement:

The Andes Biodiversity and Ecosystem Research Group (ABERG) is a team of researchers dedicated to understanding biodiversity, species distribution, and ecosystem function in the Peruvian Andes. ABERG is committed to data exchange within the scientific community and promoting collaboration among other tropical ecosystem scientists. For more information and to request data, contact Miles Silman (http://www.andesconservation.org/). The ABERG wood density dataset used in our study is deposited in the Zenodo digital repository (https://doi.org/10.5281/zenodo.10864740). Global Wood Density Data Base was extracted from the Dryad repository (https://doi.org/10.1111/j.1461-0248.2009.01285.x). The RAINFOR forest plots data was extracted from the ForestPlots database (https://forestplots.net/).

Abstract

1. Understanding how functional traits are related to species diversity and ecosystem properties is a central goal of ecology. Wood density is a trait that integrates many aspects of plant form and function and is highly variable among species. Previous studies of wood density across elevational gradients have been based on limited sampling and have reported declines with increasing elevation, though even this simple pattern remains unknown, much less its underlying functional and evolutionary relationships.

2. Here, we use one of the longest and most speciose elevational gradients in the world, extending from the Andean tree line to the Amazon basin, to test the extent to which elevation, species composition, phylogenetic affinity, and forest structure determine variation in wood density. Using field-collected wood samples and global databases, we assigned wood density to 1231 species and 31,330 stems across 41 (47.5 ha) mature forest plots arrayed across a 3,500 m vertical gradient.

3. Our results show that mean wood density, either weighted by abundance, basal area, or species, was highly variable but tended to decline from low to middle elevations and increase again from mid-elevations to the tree line. As a result of this non-linearity, forests at the Andean tree line had higher wood density than their lowland Amazon counterparts. We observed an abrupt transition in wood density at the lower limit of persistent cloud formation (cloud base), where the lowest wood density values were found. The decline of wood density is attributed to a significant shift in life forms, with an abundance of tree ferns at middle elevations and a higher probability of landslides and disturbances favoring a suite of traits associated with low wood density, such as softer wood and higher elasticity. Species turnover explained most of the

among-species variation across the gradient, with elevation having no consistent effect on within-species variation in wood density.

4. Together, both gradual compositional changes and sharp local changes in the importance of non-dicot life forms, such as arborescent ferns and palms, define patterns of forest-level carbon density, with wood density *per se* controlling ecosystem properties across the Andes-to-Amazon elevational gradient.

Keywords: Amazon, Andes, elevational gradient, functional trait, species composition, wood density

Introduction

Understanding how functional traits are related to species diversity and ecosystem properties is a central goal of ecology, and it is also important to understand ecosystem services, biodiversity conservation, and ecosystem responses to global change (Asner *et al.*, 2016; Neyret *et al.*, 2016; Fyllas *et al.*, 2017). Climate and landscape gradients are efficient natural laboratories for investigating the environmental controls on ecosystem function and diversity (von Humboldt, 1838; Malhi *et al.*, 2010). Among natural gradients, the Amazon-Andes region is among the longest environmental gradients and contains the most diverse and complex forests globally (Gentry, 1995; Silman, 2014). In this study, we focus on the basic wood-specific gravity (hereafter wood density) as an integrating functional trait of the ecosystem that can capture the influence of environmental variables (e.g., temperature and moisture), forest architecture, and mechanical characteristics along elevational gradients (Sperry, Meinzer and McCulloh, 2008; Chave *et al.*, 2009). Understanding variations in wood density can give insights into tree life history strategies, growth rate, and the role of climate and disturbance in tree demography (Putz *et al.*, 1983; Swenson and Enquist, 2007; Poorter *et al.*, 2008; Adler *et al.*, 2014).

Inter- and intraspecific wood density variability

Wood density is a functional trait that varies between species, within species, and within individual ecological functions. Inter- and intraspecific variation in wood density is closely related to diameter growth rate (Putz *et al.*, 1983; Muller-Landau, 2004; King *et al.*, 2005), hydraulic properties of the plant (Zanne *et al.*, 2010), and other wood properties such as porosity, resistance, and the number of vessel cells (Chave *et al.*, 2009; Fortunel *et al.*, 2014). At the community level, variation in wood density is often related to forest successional stage and life

history trade-offs between light-demanding and shade-tolerant species. Fast-growing and light-demanding species typically have lower wood density values than shade-tolerant species (Chave *et al.*, 2009), though the variability in the relationship between the rate of growth and wood density is high and subject to multidimensional trade-offs (Rüger *et al.*, 2012) with some fast-growing species have the highest wood density values recorded in tropical forests (e.g., *Tabebuia* spp.). The importance of within-species variation in wood density vs. among-species variation is critical to understanding the community-level importance of wood density and its implication in ecosystem functioning. Even less understood are the differences in wood density among life forms, e.g., true trees vs. arborescent life forms without secondary xylem (e.g., palms and tree ferns). Varying abundances of these life forms are likely to affect ecosystem-level attributes such as carbon storage.

Wood density variation across tropical environmental gradients

Existing studies of tropical forests across geographic and environmental gradients suggest high variation in wood density within and among tree communities (Williamson, 1984; Fortunel *et al.*, 2014). For example, across the Amazon basin, wood density is higher in the central and eastern Amazon than in northwestern Amazonia, both at the species level (Muller-Landau, 2004; Chave *et al.*, 2006) and stand level per stem basis (Baker *et al.*, 2004). This pattern can be explained by the disproportionate abundance and diversity of taxa with high wood density values associated with poor soils found in central and eastern Amazonia (Baker *et al.*, 2004; Muller-Landau, 2004; ter Steege *et al.*, 2006). However, there is still uncertainty about whether these patterns are caused by changes in wood density within all species in a community or, as tree communities comprise a few abundant species and many rare species (Pitman, Silman and

Terborgh, 2013; ter Steege *et al.*, 2013). Patterns may be driven by hyperdominants or oligarchs—species that combine high local density with broad distributional ranges in Amazonia.

Of all the gradients in the Neotropics, the forested gradient from the tropical high Andes to Amazonian lowlands has the largest functional diversity and species richness and is likely the highest-richness and plant functional diversity gradient on Earth (Asner *et al.*, 2016). Though wood density is a key functional trait that links plant diversity with ecosystem function in tropical forests, our knowledge of this trait along environmental gradients in the Neotropics is incomplete, measured only at the lower end (0–2500 m) of an elevation gradient extending up to 4000 m, and only at the species level (Chave *et al.*, 2006). This leads to important questions. (1) Given that leaf canopy traits are highly variable along elevational gradients (Asner *et al.*, 2016; Neyret *et al.*, 2016), what is the pattern of wood density variation? (2) How is wood density related to elevation *per se*, as indicated by within-species variation based on environmental changes vs. turnover in species—and even deeper phylogenetic conservatism?

We investigated the variation of wood density as a functional trait in an elevational gradient spanning ~3500 m from the Andean tree line to the Amazon basin on the eastern slope of the Peruvian Andes. To our knowledge, this is the first study in the Neotropics that assesses changes in wood density on an extensive elevational gradient using both field-collected wood samples and plot-based sampling approaches, including trees, palms, and tree ferns. We ask (1) what is the pattern of intra- and inter-specific variation in wood density across the Andes-to-Amazon gradient?; (2) What is the effect of elevation on community wood density variation and distribution, and how does this pattern differ when communities are defined by species composition and stem abundance?; (3) What is the relationship between wood density and stem size across the elevation gradient?

Methods

Study site and climate

The study was performed on the eastern slope of the Peruvian Andes along an elevational gradient extending from the Andean tree line at 3700 m to the Amazon basin at 190 m in the Manu Biosphere Reserve (11.8564° S, 71.7214° W) and Tambopata National Reserve (12.9206° S, 69.2819° W). Mean annual temperature decreases linearly along the gradient with increasing elevation at a lapse rate of 5.2 ºC/km, ranging from ~27 ºC at the lowest elevations to ~6 ºC at the tree line (Rapp and Silman, 2012; Malhi *et al.*, 2016). Mean annual precipitation varies across the gradient from 2448 to 5500 mm yr^{-1}, with significant inter-annual variability (Rapp and Silman, 2012; Malhi *et al.*, 2016). There also is distinct seasonality in rainfall, with the highest rainfall in January and February and the lowest in June and July. Winds vary little throughout the year, with the dominant pattern being upslope winds during the day and downslope winds at night (Rapp and Silman, 2012). The study area has high cloud frequency in contrast to many other areas of the eastern slope of the Andes, with clouds present in all seasons. Along the elevational gradient, the cloud base zone is estimated to be between 1500–2000 m, with the highest mean annual cloud frequency between 2000–3500 m (Halladay, Malhi and New, 2012).

Wood density calculation

We focused sampling on the dominant montane forest species because they are poorly or unrepresented in global databases. In our study area, we have registered 908 arborescent species above 1000 m elevation, and our field-taken wood samples comprise 34% of those species. We

collected wood cores from 892 individuals representing 311 species of the dominant arborescent life forms—including trees, tree ferns (hereafter ferns), and palms from 2009 to 2015. We stratified sampling of wood cores across the gradient to ensure coverage of a broad range of taxa and to collect at least one individual for every species at each elevation. Core samples were collected in 51 sites ranging from 346 to 3650 m of elevation (Fig. 1). An increment borer was used to extract wood core samples for trees and palms ≥10 cm diameter at breast height (DBH). The DBH of the sampled individuals ranged from 10 to 85 cm, and core samples were extracted from 1 to 1.3 m above the ground. For trees and palms, the wood cores were taken from the heartwood to the bark to capture density variation within the trunk. For arborescent ferns, sliced samples were taken from the trunk-like rhizomes in six different sections, and the average density value of the individual was used. Core samples were taken from individuals of targeted species outside of the permanent plots across the gradient (see below "inventory plot data" section) to avoid effects on plants that are part of long-term studies.

All values here are reported as a *wood basic specific gravity*, which is defined as oven-dry mass divided by its green volume (Fearnside, 1997; Chave *et al.*, 2006; Williamson and Wiemann, 2010) and henceforth called *wood density* in the text for simplicity. Wood density was calculated using the water displacement method with all samples oven-dried to constant mass and weighted to the nearest 0.001 g (Chave *et al.*, 2006). Values of wood density were first calculated at oven-dry temperature at ~80 ° C. Because of the possible presence of bond water in the wood samples (Williamson and Wiemann, 2010), we used a sub-sample (n = 145) to calculate wood density at 105 °C. We developed a correction equation (105 °C WD = - 0.0113 + 0.9969 × 80 °C WD; Fig. S1) that was applied to calibrate the wood density values of the rest of the wood samples. We observed no significant difference among the wood density values at 105

235 ºC and 80 ºC (Mann-Whitney-Wilcoxon test, n = 145, $p = 0.31$). The overall mean difference
236 between wood density values at 105 ºC and 80 ºC was 2.4 % ± 0.38 (95 % CI).
237
238 *Inventory plot data*
239 Plot data were collected from 41 (47.5 ha) permanent mature forest plots across an
240 elevation gradient ranging from 190 to 3625 m elevation, extending from lowlands through the
241 montane forest up to the Andean tree line. A network of 24 1-ha permanent plots was established
242 and monitored by the Andes Biodiversity and Ecosystem Research Group—ABERG ranging
243 from 387 to 3625 m elevation (ABERG PlotData, 2020). Additionally, 17 (23.5 ha) permanent
244 plots were established by various investigators in lowland forests and are now monitored by the
245 Amazon Forest Inventory Network—RAINFOR (Fig. 1). The RAINFOR plot data were
246 extracted from the ForestPlots.net database (Lopez-Gonzalez *et al.*, 2011). The permanent forest
247 plots contain 31,330 stems greater than 10 cm DBH and encompass 1,950 species (of which 35%
248 are morphospecies). Overall, the registered species in the transect belonged to 408 genera and
249 111 families (*sensu* APG IV).
250
251 *Botanical identification*
252 All botanical vouchers taken with the wood core collections were identified and then
253 compared and standardized with the permanent forest plots vouchers that were deposited in the
254 Peruvian and USA herbaria (CUZ, HUT, MOL, USM, and DAV, MO, F, and WFU,
255 respectively). Additionally, local flora and plant checklists were used as references (Pennington,
256 Reynel and Daza, 2004; Farfan-Rios *et al.*, 2015; Vasquez M. and Rojas G., 2016), and plant
257 identifications were also confirmed by taxonomic experts. The APG IV classification (Chase *et*

al., 2016) was followed for the taxonomy names, and the Taxonomic Name Resolution Service (TRNS) online application was used to standardize scientific plant names (Boyle *et al.*, 2013).

Data analysis

We analyzed wood density interspecific variation against elevation using each individual of a given species sampled in the field. A restricted maximum likelihood (REML) analysis was used to test the inter-specific variance of wood density across phylogenetic levels along the gradient (Messier, McGill and Lechowicz, 2010). Variance partitioning analysis was done using the *lme* and *varcomp* functions in R where a generalized linear model was fitted to the variance across four scales nested levels: *species*, *genus*, *family*, and *plot*. Variance partitioning allowed us to test the role of phylogeny and plot-to-plot variability including elevation. To test the effect of elevation on intra-specific variation in wood density, we used a subset of the field-collected samples. We used 46 species with ≥5 individuals that were present at least in two research sites along the gradient. We then calculated the slopes of the linear regression models for each of the selected species to observe the distribution of slopes and assess the positive, negative, or non-relationship with elevation.

To analyze wood density variation across the elevational gradient at the plot level, we calculated an average species wood density value derived from the wood samples collected in the field (311 species, 892 individuals), and those values were assigned to each stem of a given species in the plot network across the transect. For stems with no measured density values from the transect, we incorporated wood density values from the Global Wood Density Data Base (Zanne *et al.*, 2009). Overall, we compiled 1,231 forest taxa from field-collected samples and published resources (Table S1). When density values were unavailable from the combined

datasets of field-published resources at the species level, the mean values at the genus or family level were used. This was the case for the unidentified individuals to a species level (morphospecies) that accounted for 13% of the total individuals. The local plot-level mean value was used for the unknown taxa (0.8% of all taxa). We then calculated the mean wood density of each plot in two ways. First, we calculated the average wood density across all species present in each plot (species mean WD), and then we calculated the mean wood density by weighting each species by its number of stems (stem-weighted WD). In addition, species mean WD was also weighed by basal area. We ran the analysis for all arborescent life forms (i.e., trees, ferns, and palms) and for trees only, and in all the cases, we excluded lianas from the analysis. The outcome of this analysis indicates the influence of the arboreal life forms, the number and size of stems, and the species composition turnover on plot-level wood density variation along the elevation gradient.

To allow biogeographical comparations of wood density along the elevational gradient, the plots were divided into five different forest types corresponding to those existing in the literature (Young, 1992; Pennington, Reynel and Daza, 2004): *Lowland* (≤500 m; including *terra firme*, *floodplain,* and *bamboo dominated*), *submontane* (500–1500 m), *lower montane* (1500–2500 m), *upper montane* (2500–3400 m), and *tree line* (≥3400 m). Finally, wood density variation was calculated across diameter classes to compare forest structure across forest types. We used ordinary least squares linear regression to explore the intra-and inter-specific relationships between wood density and elevation and the smoothing function of a generalized additive model (GAM) to fit response curves and to test the relationship between wood density and elevation if a non-linear relationship was observed.

Results

Across the entire elevational gradient, species mean WD for all arborescent life forms was 0.578 g cm^{-3} ± 0.004 (95% CI). Focusing on single life forms, the dicot tree species' mean WD was 0.587 g cm^{-3} ± 0.004 (95% CI), for palms were 0.410 g cm^{-3} ± 0.026 (95% CI), and for arborescent ferns were 0.351 g cm^{-3} ± 0.003 (95% CI). The maximum wood density value was 1.120 g cm^{-3} for *Machaerium acutifolium* (Fabaceae) in the submontane forest, and the minimum value was 0.111 g cm^{-3} for *Erythrina ulei* (Fabaceae) in the lowland forest. The mean stem-weighted WD for all life forms at the plot level was 0.547 g cm^{-3} ± 0.002 (95% CI), and the means for trees, palms, and ferns were 0.584 g cm^{-3} ± 0.001 (95% CI), 0.347 g cm^{-3} ± 0.004 (95% CI) and 0.349 g cm^{-3} ± 0.008 (95% CI), respectively. Across all elevations, the overall distribution of species and stem-weighed WD for all arborescent life forms and trees alone was symmetric and normal but with a slight positive skewness and kurtosis for species WD and negatively skewed for stem-weighed WD (Supporting information, Fig. S2).

Inter- and intra-specific variation of wood density along elevation

Variance partitioning showed that evolutionary relatedness explained most of the variance in wood density for both species sampled in the field (69.4% of the variation) and the plot level, including the 41 forest plots (99.7% of the variation) across the gradient (Fig. S3). The differences among families accounted for the largest proportion of the total variation for the field-sampled species (28.5%), and at the plot level the largest variation was among genera (47.1%; Fig. S3).

For the relationship of intraspecific variation in wood density with elevation, 83% of the species sampled (n = 46, ≥5 individuals) showed no relationship with elevation, and only eight species showed a significant response (Fig. 2a). We found that the modal slope from the

regressions was essentially zero [n = 46, $\bar{x}$ = 0.0003 ± 0.0001 (95% CI)], with a slight bias toward positive regression slopes (increasing intraspecific wood density with increasing elevation), as compared to negative slopes, with only eight slopes significantly different from zero (Fig. 2a). However, we found large variation between tree species in both the sign and strength of the relationship. For example, wood density in *Clethra cuneata* shows a highly significant decrease with increasing elevation (n = 45, $F_{1,43}$ = 18.44, adj. R^2 = 0.28, $p < 0.0001$; Fig. 2b), whereas *Morella pubescens* (n = 20, $F_{1,18}$ = 2.90, adj. R^2 = 0.09, p = 0.11; Fig. 2c) and *Weinmannia bangii* (n = 26, $F_{1,24}$ = 0.0004, adj. R^2 = 0.00, p = 0.98; Fig. 2d) had no relationship with elevation. The wood density of *Alnus acuminata* (n = 17, $F_{1,15}$ = 7.75, adj. R^2 = 0.30, p = 0.013; Fig. 2e) and *Weinmannia fagaroides* both increased significantly with increasing elevation (n = 28, $F_{1,26}$ = 10.55, adj. R^2 = 0.26, p = 0.003; Fig. 2f).

Plot-level wood density variation along the elevational gradient

Across the Andes-to-Amazon gradient, plot-to-plot mean wood density showed a non-linear relationship with elevation (Fig. 3, Table S1, Fig. S4). Species mean WD for all arborescent life forms decreased slightly from 190 to 1500 m and remained constant from 1500 to 2500 m, subsequently increased linearly up to the tree line at ~3650 m (Fig. 3a). This trend was different when considering only tree species, with wood density decreasing from 190 to 1500 m and linearly increasing above cloud base up the tree line; palms and fern species mean wood density did not show a relationship with elevation (Fig. 3b, S5). Stem-weighted WD for all arborescent life forms remained constant until 2000 m, declined abruptly between 2250 and 2500 m, and then increased with elevation (Fig. 3c). This trend changed for trees only, with stem-weighted WD slightly declining until the cloud base and then increasing up to the tree line (Fig. 3d). Palm and fern stem-

weighted WD were not related to elevation (Fig. 3d, S5). The influence of life forms on plot-level mean wood density variability was driven at middle elevations by arborescent ferns and by palms in lowland sites (Fig. 3, Table S1). When mean species level wood density was weighted by basal area, weighted species mean WD for all arborescent life forms showed lower values, and the stem-weighted WD for trees showed a stronger non-linear relationship of wood density with elevation (Fig. 4a, b), with the lowest values recorded in the submontane forest (Fig. 4b). Species mean wood densities obtained using genus- and family-level identification were highly correlated with those using species-level data ($p < 0.0001$, r = 0.94; $p < 0.0001$, r = 0.89 respectively; Fig. S6).

We observed that plot-to-plot wood density distributions and their statistical moments varied across elevation for both species and stem-weighted WD (Fig. 5). The species WD skewness did not show a clear pattern from low to high elevations. However, the skew was more pronounced at the middle and low elevations for stem-weighted WD, indicating a clear influence of the abundance of low wood density taxa (Fig. 5; Table S2). Mean wood density differs significantly among forest types at the species and stem level (Fig. 6 a-b), but the difference for stem-weighted WD for all arborescent life forms was not significant among life zones along the gradient (Fig. 6 c-d; Kruskal-Wallis, n = 7; species WD for all arborescent life forms, $x^2 = 16.19$, $p = 0.013$; for trees, $x^2 = 15.35$, $p = 0.018$; stem-weighted WD for all arborescent life forms, $x^2 = 11.62$, $p = 0.071$; for trees, $x^2 = 15.67$, $p = 0.016$). For all taxa, species mean WD was lower at low elevations, reaching a minimum below cloud base in submontane forests and increasing through tree lines for all life forms and trees alone (Fig 6a, b). Stem-weighted WD remained constant toward the lower montane forest and increased only in the upper and tree line forests. When growth form was restricted to just trees, the pattern shifts, with a distinct drop in wood density in

372 submontane forests and wood density exceeding its lowland values only in upper-montane and
373 tree line forests (Fig. 6c, d).
374
375 *Wood density and forest structure*
376 Although the relationship between wood density and DBH class varies greatly among
377 forest types along the gradient, we observed a general tendency where mean wood density
378 decreases with DBH across forest types, and that trend was significant in the submontane (n = 5,
379 $F_{1,3}$ = 22.46, adj. R^2 = 0.84, p = 0.018) and lower montane (n = 5, $F_{1,3}$ = 12.69, adj. R^2 = 0.74, p =
380 0.037) forests (Fig. 7a). Only in the bamboo-dominated forest mean wood density increased across
381 DBH classes (Fig. 7a). The relationship of mean wood density and DBH classes follow different
382 patterns across the elevation and between the forest plots with stark variability for big trees over
383 50 cm DBH in lowlands (floodplain and terra firme forests) and lower montane forests plots (Fig.
384 7b).
385
386 **Discussion**
387 Mean wood density changes substantially from lowlands to montane environments across
388 the Andes-to-Amazon elevational gradient. Plot-level mean wood density showed a clear non-
389 linear relationship with elevation, and that pattern is explained by changes in species
390 composition and species sorting based on local conditions rather than any general direct effect of
391 elevation *per se,* with intraspecific variation in wood density being absent or showing no
392 consistent trend with elevation. We observed that most of the wood density variation was a result
393 of among-species differences and differences in the community composition because of changes
394 in the relative abundances of different arborescent life forms rather than any within-species

variability across the elevational gradient. Moreover, the abundance and distribution of arborescent ferns and palms had a large effect on mean wood density values along the gradient, decreasing wood density by 21% in montane forests dominated by tree ferns and 16% in lowland forests dominated by palms. When looking at community-level changes, the means and distributions of wood density differed greatly depending on whether species were weighted equally or whether wood density values were weighted by individual (community-weighted mean density). To better understand community-level functional traits and their ecological importance, species lists from plots by themselves are not enough, and they need to be combined with the number of individuals and stem size (basal area).

Non-linear relationship of increasing wood density with elevation

The present study provides a new framework to understand how wood density varies at species and stem levels across forest types and along a broad elevational gradient. In contrast to the current study, a previous study suggested that wood density significantly decreased with increasing elevation (Chave *et al.*, 2006). The discrepancy could be because Chave et al. (2006) only evaluated wood density from 0 to 2500 m rather than the entire Andes-to-Amazon gradient spanning 190 to 3650 m of elevation. Although species mean wood density declines slightly with increasing elevation up to ~1500 m, it increases above that up to the tree line (Fig. 3, 6).

The non-linear relationship between wood density and elevation (Fig. 3) is the result of species composition turnover and environment filtering of life histories based on wood density or traits associated with wood density rather than a physiological response (intraspecific variation) to the elevation gradient, which is reflected in the decrease of the distributional variance with increasing elevation at species- and stem-weighted WD (Table S2). The variation in species

mean WD resides predominately at genus- and family-level, and that variation principally occurs between rather than within genera and families (Fig. S3), indicating that wood density is highly conserved phylogenetically (Chave *et al.*, 2006; Swenson and Enquist, 2007). The same phylogenetic pattern has been found for leaf mass per area measured from forest canopies across an Andean elevational gradient (Neyret *et al.*, 2016), as well as a large suite of leaf functional traits (G. P. Asner *et al.*, 2014), demonstrating that a wide range of plant functional traits is evolutionarily conserved. We know this is true for individual traits but understanding the correlated suites of traits—the covariances among them—would give information about the major axes of variation or syndromes of functional traits if they do exist (Asner *et al.*, 2016; Díaz *et al.*, 2016). This is important in understanding the effects of environmental filtering and lineage sorting in shaping functional trait patterns across environmental gradients and raises questions about the relative influences of historical (e.g., Andean uplift) and ecological forces in shaping functional traits variation in tropical forests (Chave *et al.*, 2006).

Wood properties and the increase of wood density with elevation

Whereas wood density is taken as a comprehensive functional trait, wood has many functions and properties, and only some of them are correlated with density. For instance, non-lumen tissue, such as vessel walls, fibers, and parenchyma, only explain 15% of the variation in wood density, and vessel lumen fraction is unrelated to wood density (Zanne *et al.*, 2010)—what selective forces drive vessel and fiber trait variation remains unclear. Colder environments are potentially dominated by taxa that contain small vessels and tracheids that probably evolved before climate occupancy (Tyree and Zimmermann, 2002; Zanne *et al.*, 2014). Forests at tree lines are exposed to air temperatures below 0 ^{o}C and can reach $\leq$-5 ^{o}C in the austral dry season

(June), exposing plants to freezing conditions (Rapp and Silman, 2012). Thus, it is expected that these taxa will contain numerous but short vessels with narrow diameters (Wheeler, Baas and Rodgers, 2007) and thick-walled fibers and vessels (Chave *et al.*, 2009) explaining the high wood density values at higher elevations. In addition, wood density has shown an evolutionary correlation with other plant traits. For instance, wood density decreases with increasing leaf size but was found to be generally unrelated to other functional traits such as seed size, fruit size, and plant height (Wright *et al.*, 2007). However, there are mixed findings for the wood density and leaf mass per area (LMA) relationship, showing either a positive relationship (Ishida *et al.*, 2008) or none at all (Wright *et al.*, 2007). Along a tropical elevational gradient, LMA increases linearly with increasing elevation (Asner *et al.*, 2016), suggesting a positive relationship between wood density and LMA in the Manu-Tambopata elevational transect, although this remains untested. The complex relationships between wood and leaf function remain unclear but are important to understanding the leaf-wood construction costs in the plant growth spectrum between conservative and acquisitive species.

Dominant taxa and life forms control wood density variation across the gradient

The role of dominant taxa and arborescent life forms impacts the observed patterns of stem-weighted WD variation across the gradient (Fig. 3, 5, 6). Trends of species and stem-weighted WD with elevation for all arborescent life forms were highly nonlinear (deviance explained = 57.5% for species and 36.4% for stem-weighted WD; Fig. 3a c, S5), and this relationship is even stronger for stem-weighted WD when palms and ferns are excluded (deviance explained = 39.7%; Fig. 3d, S5). The non-linear but positive relationship between wood density and elevation can be explained by the increase in the dominance of heavily

464 wooded species at higher elevations (sensu Slik et al., 2010). More generally, forests at the tree
465 line are dominated by taxa with higher wood density than their lowland counterparts, with lowest
466 values at middle elevations (Figs. 3, 5, 6). For instance, the ten most dominant species at our
467 highest plot in the tree line (e.g., *Miconia alpina*, 0.740 g cm^{-3}) account for 17% of the total
468 species but hold 70% of the total stems. This indicates that the highest values of stem-weighted
469 WD at higher elevations (Figs. 3 c, d) are driven by a few dominant heavy-wooded species.
470 Contrasting with the montane pattern, in the Amazonian floodplain forest, the ten most dominant
471 species (e.g., *Iriartea deltoidea* 0.265 g cm^{-3}), even though accounting for only 2% of the total
472 species, they account for 38% of the total stems. If we exclude these dominant species, mean
473 wood density values of the floodplain forests show a nonsignificant increase from 0.522 to 0.557
474 g cm^{-3} (Mann-Whitney-Wilcoxon test, n = 6, p = 0.132). This suggests that the abundance of
475 these few species could explain the lower mean stem-weighted WD found in floodplains and, in
476 general, in lowland forests. The plot-level variability in mean species and stem-weighted WD in
477 the Amazonian forest (Fig. 3, 6) can also be associated with the difference in the geomorphology
478 between the Holocene (floodplain) and Pleistocene (terra firme) sediments (Phillips *et al.*, 2019).
479 Whereas general trends in mean wood density values were clear across the elevation
480 gradient, there is substantial variability within any elevation, and much of this variation can be
481 accounted for by the abundance of different arborescent life forms. Dicot trees were the
482 dominant group along the gradient; however, arborescent ferns (i.e., Cyatheaceae and
483 Dicksoniaceae) and palms (i.e., Arecaceae) had large effects on mean plot wood density
484 variation in lower montane and lowland forests (Figs. 3, 5, S5). For example, the abrupt decline
485 of mean stem-weighted WD in the submontane and lower montane forests (Figs. 3 a,c; 5; 6 a,c)
486 in the Manu-Tambopata elevational transect is explained by the high abundance of ferns (mean

wood density 0.35 g cm^{-3}) at middle elevations. Excluding the dominance of arborescent ferns in the montane forest, mean stem-weighted WD significantly increases from 0.542 to 0.585 g cm^{-3} (Mann-Whitney-Wilcoxon test, n = 13, $p = 0.04$), but that difference is pronounced in some sites, for example in TRU-05 and TRU-06 plots, where arborescent ferns comprise 52% and 48% of the total stems at each plot, respectively, resulting in a 24% (for TRU-05) and 20% (for TRU-06) difference in stem-weighted WD as opposed to unweighted WD (Table S1). The same fern abundance patterns at the plot level were found at middle elevations in the Costa Rica elevational transect (Lieberman *et al.*, 1996), indicating that the high abundance of this functional group has important effects on forest structure that translates to the carbon cycle in Neotropical montane forests.

The lowest wood density and forest disturbance

Arborescent life forms have profound effects on the wood density variation across the elevation gradient, but this does not fully explain why wood density is lower in mid-montane forests near the cloud base. Excluding non-tree life forms, plot-to-plot wood density variation in true trees (those with secondary xylem) still follows the non-linear relationship along the gradient (Fig. 3, 6; S5). Forest dynamics in tropical mountains are highly influenced by natural disturbances with significant effects on the forest structure, diversity, and function (Crausbay and Martin, 2016). Landslides and tree gaps may be the primary driving forces for vegetation turnover and changes in tree species composition in Andean tropical mountains. Accordingly, a plausible explanation for the consistent trends of lower values of mean wood density at middle elevations around the cloud base may be due to the effects of landslide occurrence. It has been shown that high landslide probability occurs at ~1500 m of elevation (Clark *et al.*, 2015; Freund

510 *et al.*, 2021) just below and including the cloud base—below the cloud immersion zone—in the
511 study area (Halladay, Malhi and New, 2012). These are elevations with exceptionally high
512 rainfall, with rain gauges at the site measuring 6–10.5 m of rain per year at 1400 m and 4–8.8 m
513 yr of precipitation at 1800 m. The size, intensity, and recurrence of landslides around the cloud
514 base may lead to a high tree species turnover, facilitating the establishment of fast-growing
515 species with low wood density (e.g., *Urera caracasana*, 0.180 g cm^{-3} and *Heliocarpus*
516 *americanus*, 0.215 g cm^{-3}), resulting in highly dynamic and heterogeneous forests with high
517 abundances of low wood-density species. Even large trees have significantly lower wood density
518 values in the sub and lower montane forests than their lowland and upland counterparts (Fig. 7).
519 The light-woodedness may be due to the demands of establishing on high-turnover and
520 competitive landscapes, but it also may be related to the exceptional quantity of precipitation and
521 clouds and low VPD, making large vessel and light-woodedness possible, even for large trees. A
522 way to differentiate between the hypotheses would be to look at the multivariate trait spectrum
523 and see if other traits associated with regeneration on disturbed landscapes are higher at these
524 elevations. In either case, the relationship between minimum mean community wood density
525 with high landslide frequency may be important in understanding how tree communities are
526 assembled.
527
528 *Ecosystem consequences*
529 Wood density has been suggested to play a key role in understanding ecosystem
530 properties, such as carbon cycling (Zanne *et al.*, 2010), and is considered one of the six
531 functional traits that bridge tree diversity and ecosystem function (Díaz *et al.*, 2016). To improve
532 aboveground carbon estimations in tropical forests, allometric equations now include wood

density values to reduce uncertainties because it is critical to capture spatial patterns of carbon dynamics at local and regional scales (Malhi *et al.*, 2006; Phillips *et al.*, 2019). Here, we provide a wood density database to reduce uncertainties in carbon calculations, particularly for Andean montane forests where biomass declines with elevation (Asner et al., 2014; Malhi et al., 2016). Current aboveground biomass estimates across the Amazonian forests include palm communities in their calculations (Asner et al., 2014; Malhi et al., 2006). However, even though tree fern abundance exceeds 50% of stems per hectare in some elevations, they are not included in global tropical forest carbon estimates (Saatchi *et al.*, 2011), excluding their contributions to tropical forest carbon stocks. This reinforces the importance of including all arborescent life forms in global forest biomass calculations.

This study provides insights into how wood density variation among functional groups, stem size, and habitats could improve carbon dynamic calculations in tropical forests. The sizes of trees (i.e., stem diameter) are important in biomass calculations, in particular, large rainforest trees that account for 2% of the stems but store up to 40% of aboveground biomass per hectare (Clark and Clark, 1996). In this study, when wood density was weighted by basal area, the values were lower than the unweighted wood density, suggesting the dominance of species with low wood density in large sizes trees (Fig. 4). We also observed that large size trees across the gradient tended to have lower mean wood density values that small size classes in all forest types except for bamboo-dominated forest (Fig. 7, S7). Large trees with the lowest wood density values were coincidentally found in the submontane forest, where the lowest community wood density was reported. This negative correlation between wood density and stem diameter was also found in Thai (Sungpalee *et al.*, 2009) and Panamanian tropical forests (Chave *et al.*, 2004); however, the causality of this trend has yet to be resolved.

Even though we have expanded the wood density dataset and the understanding of how wood density varies across a 3.5 km elevation gradient, basic uncertainties remain. Even in the most intensive and taxonomically rigorous surveys of tropical Andean forests, 20–40% of taxa (among different Andean surveys) remain as morphospecies known only at the genus level, hampering regional and biogeographic comparisons as well as the understanding of the evolutionary pressures shaping wood density. However, as more than 65% are identified species, it gives us insights into wood density variation across the Andes-to-Amazon forests and contributes to understanding the effects of wood density (species composition) on ecosystem function in particular when projecting future patterns of carbon dynamics based on projected climate changes.

References

ABERG PlotData (2020) ‘Permanent forest plot network’, *http://www.andesconservation.org/* [Preprint].

Adler, P.B. *et al.* (2014) ‘Functional traits explain variation in plant life history strategies’, *Proceedings of the National Academy of Sciences*, 111(2), pp. 740–745. Available at: https://doi.org/10.1073/pnas.1315179111.

Asner, G. P. *et al.* (2014) ‘Landscape-scale changes in forest structure and functional traits along an Andes-to-Amazon elevation gradient’, *Biogeosciences*, 11(3), pp. 843–856. Available at: https://doi.org/10.5194/bg-11-843-2014.

Asner, Gregory P. *et al.* (2014) ‘Targeted carbon conservation at national scales with high-resolution monitoring’, *Proceedings of the National Academy of Sciences*, 111(47), pp. E5016–E5022. Available at: https://doi.org/10.1073/pnas.1419550111.

Asner, G.P. *et al.* (2016) ‘Scale dependence of canopy trait distributions along a tropical forest elevation gradient’, *New Phytologist*, June. Available at: https://doi.org/10.1111/nph.14068.

Baker, T.R. *et al.* (2004) ‘Variation in wood density determines spatial patterns in Amazonian forest biomass’, *Global Change Biology*, 10(5), pp. 545–562.

Boyle, B. *et al.* (2013) ‘The taxonomic name resolution service: an online tool for automated standardization of plant names.’, *BMC bioinformatics*, 14(1), p. 16. Available at: https://doi.org/10.1186/1471-2105-14-16.

585 Chase, M.W. *et al.* (2016) ‘An update of the Angiosperm Phylogeny Group classification for the
586 orders and families of flowering plants: APG IV’, *Botanical Journal of the Linnean Society*,
587 181(1), pp. 1–20. Available at: https://doi.org/10.1111/boj.12385.

588 Chave, J. *et al.* (2004) ‘Error propagation and scaling for tropical forest biomass estimates’,
589 *Philosophical Transactions of the Royal Society B: Biological Sciences*, 359(1443), pp. 409–420.
590 Available at: https://doi.org/10.1098/rstb.2003.1425.

591 Chave, J. *et al.* (2006) ‘Regional and phylogenetic variation of wood density across 2456
592 neotropical tree species’, *Ecological Applications*, 16(6), pp. 2356–2367.

593 Chave, J. *et al.* (2009) ‘Towards a worldwide wood economics spectrum’, *Ecology Letters*,
594 12(4), pp. 351–366. Available at: https://doi.org/10.1111/j.1461-0248.2009.01285.x.

595 Clark, D.B. and Clark, D.A. (1996) ‘Abundance, growth and mortality of very large trees in
596 neotropical lowland rain forest’, *Forest Ecology and Management*, 80(1–3), pp. 235–244.
597 Available at: https://doi.org/10.1016/0378-1127(95)03607-5.

598 Clark, K.E. *et al.* (2015) ‘Storm-triggered landslides in the Peruvian Andes and implications for
599 topography, carbon cycles, and biodiversity’, *Earth Surface Dynamics Discussions*, 3(3), pp.
600 631–688. Available at: https://doi.org/10.5194/esurfd-3-631-2015.

601 Crausbay, S.D. and Martin, P.H. (2016) ‘Natural disturbance, vegetation patterns and ecological
602 dynamics in tropical montane forests’, *Journal of Tropical Ecology*, 32(05), pp. 384–403.
603 Available at: https://doi.org/10.1017/S0266467416000328.

604 Díaz, S. *et al.* (2016) ‘The global spectrum of plant form and function’, *Nature*, 529(7585), pp.
605 167–171. Available at: http://dx.doi.org/10.1038/nature16489.

606 Farfan-Rios, W. *et al.* (2015) ‘Lista anotada de árboles y afines en los bosques montanos del
607 sureste peruano : la importancia de seguir recolectando’, *Revista Peruana de Biología*, 22(2), pp.
608 145–174. Available at: http://dx.doi.org/10.15381/rpb.v22i2.11351.

609 Fearnside, P.M. (1997) ‘Wood density for estimating forest biomass in Brazilian Amazonia’,
610 *Forest Ecology and Management*, 90(1), pp. 59–87. Available at: https://doi.org/10.1016/S0378-
611 1127(96)03840-6.

612 Fortunel, C. *et al.* (2014) ‘Wood specific gravity and anatomy of branches and roots in 113
613 Amazonian rainforest tree species across environmental gradients.’, *The New phytologist*, 202(1),
614 pp. 79–94. Available at: https://doi.org/10.1111/nph.12632.

615 Freund, C.A. *et al.* (2021) ‘Landslide age, elevation and residual vegetation determine tropical
616 montane forest canopy recovery and biomass accumulation after landslide disturbances in the
617 Peruvian Andes’, *Journal of Ecology*, 109(10), pp. 3555–3571. Available at:
618 https://doi.org/10.1111/1365-2745.13737.

619 Fyllas, N.M. *et al.* (2017) ‘Solar radiation and functional traits explain the decline of forest
620 primary productivity along a tropical elevation gradient’, *Ecology Letters*. Edited by Dr.N.
621 Swenson, 20(6), pp. 730–740. Available at: https://doi.org/10.1111/ele.12771.

622 Gentry, A. (1995) ‘Patterns of diversity and floristic composition in neotropical montane
623 forests’, in S.P. Churchill et al. (eds) *Biodiversity and Conservation of Neotropical Montane*
624 *Forests: Proceedings of the Neotropical Montane Forest Biodiversity and Conservation*
625 *Symposium*. New York.: New York Botanical Garden, pp. 103–126.

Halladay, K., Malhi, Y. and New, M. (2012) 'Cloud frequency climatology at the Andes/Amazon transition: 1. Seasonal and diurnal cycles', *J. Geophys. Res.*, 117, pp. D23102, doi:10.1029/2012JD017770.

von Humboldt, A. (1838) *Notice de Deux Tentatives d'Ascension du Chimborazo (A. Pihan de la Forest, Paris)*.

Ishida, A. *et al.* (2008) 'Coordination between leaf and stem traits related to leaf carbon gain and hydraulics across 32 drought-tolerant angiosperms', *Oecologia*, 156(1), pp. 193–202. Available at: https://doi.org/10.1007/s00442-008-0965-6.

King, D.A. *et al.* (2005) 'Tree growth is related to light interception and wood density in two mixed dipterocarp forests of Malaysia', *Functional Ecology*, 19(3), pp. 445–453. Available at: https://doi.org/10.1111/j.1365-2435.2005.00982.x.

Lieberman, D. *et al.* (1996) 'Tropical forest structure and composition on a large-scale altitudinal gradient in Costa Rica', *Journal of Ecology*, 84(2), pp. 137–152.

Lopez-Gonzalez, G. *et al.* (2011) 'ForestPlots.net: a web application and research tool to manage and analyse tropical forest plot data', *Journal of Vegetation Science*, 22(4), pp. 610–613. Available at: https://doi.org/10.1111/j.1654-1103.2011.01312.x.

Malhi, Y. *et al.* (2006) 'The regional variation of aboveground live biomass in old-growth Amazonian forests', *Global Change Biology*, 12(7), pp. 1107–1138.

Malhi, Y. *et al.* (2010) 'Introduction: Elevation gradients in the tropics: laboratories for ecosystem ecology and global change research', *Global Change Biology*, 16(12), pp. 3171–3175.

Malhi, Y. *et al.* (2016) 'The variation of productivity and its allocation along a tropical elevation gradient: a whole carbon budget perspective', *New Phytologist* [Preprint]. Available at: https://doi.org/10.1111/nph.14189.

Messier, J., McGill, B.J. and Lechowicz, M.J. (2010) 'How do traits vary across ecological scales? A case for trait-based ecology', *Ecology Letters*, 13(7), pp. 838–848. Available at: https://doi.org/10.1111/j.1461-0248.2010.01476.x.

Muller-Landau, H.C. (2004) 'Interspecific and Inter-site Variation in Wood Specific Gravity of Tropical Trees', *Biotropica*, 36(1), pp. 20–32. Available at: https://doi.org/10.1111/j.1744-7429.2004.tb00292.x.

Neyret, M. *et al.* (2016) 'Examining variation in the leaf mass per area of dominant species across two contrasting tropical gradients in light of community assembly', *Ecology and Evolution*, 6(16), pp. 5674–5689. Available at: https://doi.org/10.1002/ece3.2281.

Pennington, T.D., Reynel, C. and Daza, A. (2004) *Illustrated guide to the Trees of Peru*. Edited by T.D. Pennington, C. Reynel, and A. Daza. Sherborne, UK: David Hunt.

Phillips, O.L. *et al.* (2019) 'Species Matter: Wood Density Influences Tropical Forest Biomass at Multiple Scales', *Surveys in Geophysics*, pp. 1–23. Available at: https://doi.org/10.1007/s10712-019-09540-0.

Pitman, N.C.A., Silman, M.R. and Terborgh, J.W. (2013) 'Oligarchies in Amazonian tree communities: A ten-year review', *Ecography*, 36(2), pp. 114–123. Available at: https://doi.org/10.1111/j.1600-0587.2012.00083.x.

Poorter, L. *et al.* (2008) 'Are functional traits good predictors of demographic rates? evidence from five neotropical forests', *Ecology*, 89(7), pp. 1908–1920. Available at: https://doi.org/10.1890/07-0207.1.

Putz, F.E. *et al.* (1983) 'Uprooting and Snapping of Trees - Structural Determinants and Ecological Consequences', *Canadian Journal of Forest Research-Revue Canadienne De Recherche Forestiere*, 13(5), pp. 1011–1020.

Rapp, J.M. and Silman, M.R. (2012) 'Diurnal, seasonal, and altitudinal trends in microclimate across a tropical montane cloud forest', *Climate Research*, 55(1), pp. 17–32. Available at: https://doi.org/10.3354/cr01127.

Rüger, N. *et al.* (2012) 'Functional traits explain light and size response of growth rates in tropical tree species', *Ecology*, 93(12), pp. 2626–2636. Available at: https://doi.org/10.1890/12-0622.1.

Saatchi, S.S. *et al.* (2011) 'Benchmark map of forest carbon stocks in tropical regions across three continents.', *Proceedings of the National Academy of Sciences of the United States of America*, 108(24), pp. 9899–904. Available at: https://doi.org/10.1073/pnas.1019576108.

Silman, M.R. (2014) 'Functional megadiversity.', *Proceedings of the National Academy of Sciences of the United States of America*, 111(16), pp. 5763–4. Available at: https://doi.org/10.1073/pnas.1402618111.

Slik, J.W.F. *et al.* (2010) 'Environmental correlates of tree biomass, basal area, wood specific gravity and stem density gradients in Borneo's tropical forests', *Global Ecology and*

Biogeography, 19(1), pp. 50–60. Available at: https://doi.org/10.1111/j.1466-8238.2009.00489.x.

Sperry, J.S., Meinzer, F.C. and McCulloh, K.A. (2008) 'Safety and efficiency conflicts in hydraulic architecture: scaling from tissues to trees.', *Plant, cell & environment*, 31(5), pp. 632–45. Available at: https://doi.org/10.1111/j.1365-3040.2007.01765.x.

ter Steege, H. *et al.* (2006) 'Continental-scale patterns of canopy tree composition and function across Amazonia', *Nature*, 443(7110), pp. 444–447. Available at: https://doi.org/10.1038/nature05134.

ter Steege, H. *et al.* (2013) 'Hyperdominance in the Amazonian tree flora.', *Science (New York, N.Y.)*, 342(6156), p. 1243092. Available at: https://doi.org/10.1126/science.1243092.

Sungpalee, W. *et al.* (2009) 'Intra- and interspecific variation in wood density and fine-scale spatial distribution of stand-level wood density in a northern Thai tropical montane forest', *Journal of Tropical Ecology*, 25(04), pp. 359–370. Available at: https://doi.org/doi:10.1017/S0266467409006191.

Swenson, N.G. and Enquist, B.J. (2007) 'Ecological and evolutionary determinants of a key plant functional trait: wood density and its community-wide variation across latitude and elevation.', *American journal of botany*, 94(3), pp. 451–9. Available at: https://doi.org/10.3732/ajb.94.3.451.

Tyree, M.T. and Zimmermann, M.H. (2002) 'Hydraulic Architecture of Whole Plants and Plant Performance', in *Springer*. Springer, Berlin, Heidelberg, pp. 175–214. Available at: https://doi.org/10.1007/978-3-662-04931-0_6.

Vasquez M., R. and Rojas G., R.D.P. (2016) *Clave para identificar grupos de familias de Gymnospermae y Angiospermae del Perú*. Jardin Botanico de Missouri.

Wheeler, E.A., Baas, P. and Rodgers, S. (2007) 'Variations in dicot wood anatomy: A global analysis based on the insidewood database', *IAWA Journal*. Brill, pp. 229–258. Available at: https://doi.org/10.1163/22941932-90001638.

Williamson, G.B. (1984) 'Gradients in Wood Specific Gravity of Trees', *Bulletin of the Torrey Botanical Club*, 111(1), pp. 51–55. Available at: https://doi.org/10.2307/2996210.

Williamson, G.B. and Wiemann, M.C. (2010) 'Measuring wood specific gravity...correctly', *American Journal of Botany*, 97(3), pp. 519–524. Available at: https://doi.org/10.3732/ajb.0900243.

Wright, I.J. *et al.* (2007) 'Relationships among ecologically important dimensions of plant trait variation in seven neotropical forests', *Annals of Botany*, 99(5), pp. 1003–1015. Available at: https://doi.org/10.1093/aob/mcl066.

Young, K.R. (1992) 'Biogeography of the montane forest zone of the eastern slopes of Peru', *Memorias del Museo de Historia Natural U.N.M.S.M.*, 21, pp. 119–154.

Zanne, A.E. *et al.* (2009) 'Data from: Towards a worldwide wood economics spectrum', *Ecology Letters* [Preprint]. Dryad Data Repository. Available at: http://dx.doi.org/10.5061/dryad.234.

Zanne, A.E. *et al.* (2010) 'Angiosperm wood structure: Global patterns in vessel anatomy and their relation to wood density and potential conductivity.', *American journal of botany*, 97(2), pp. 207–15. Available at: https://doi.org/10.3732/ajb.0900178.

Zanne, A.E. *et al.* (2014) 'Three keys to the radiation of angiosperms into freezing environments.', *Nature*, 506(7486), pp. 89–92. Available at: https://doi.org/10.1038/nature12872.

Figure legends:

Figure 1. Location of the 51 wood collection sites (red circles) and the 41 permanent forest plots (yellow squares) on the eastern slope of the Peruvian Andes along an elevational gradient extending from the tree line at 3700 m to the Amazon basin at 190 m.

Figure 2. (a) Empirical distribution of within-species slopes of the linear regression between wood density and elevation (n = 46)—vertical bars represent the slopes significantly different from zero (8 positives and 1 negative). Intraspecific variation in wood density across elevations for (b) *Clethra cuneata* (n = 45), (c) *Morella pubescens* (n = 20), (d) *Weinmannia bangii* (n = 26), (e) *Alnus acuminata* (n = 17), and (f) *Weinmannia fagaroides* (n = 28). Gray circles represent sampled individuals across elevation, black circles represent the mean wood density among species at each sampled site. The black solid line represents the linear regression fit with 95% confidence limits. Error bars depict bootstrapped 95% confidence intervals.

Figure 3. Plot-level mean wood density variation across 41 permanent forest plots along the Andes-to-Amazon elevational gradient for (a) species mean wood density for all arborescent life forms and (b) for trees, palms, and ferns species. (c) Stem-weighted mean wood density for all arborescent life forms and (d) for trees, palms, and ferns. Error bars depict bootstrapped 95% confidence intervals. Solid lines are generalized additive models (GAM) fit using a smoothing

function with 95% confidence limits. Vertical dashed lines represent the approximate elevation of the cloud base.

Figure 4. (a) Species mean wood density for all arborescent life forms and trees. (b) Species mean wood density for all arborescent life forms and trees weighted by basal area. Open triangles represent all arborescent life forms, and gray circles represent trees. Solid and dashed lines are generalized additive models (GAM) fit using a smoothing function. Vertical dashed lines represent the position of the cloud base along the gradient. Legend corresponds to the same life forms for panels (a) and (b).

Figure 5. Wood density distribution for species (blue lines) and stems (red lines) for all plots (n = 41) across the Andes-to-Amazon elevational gradient. Data include all arborescent life forms. Vertical dashed lines indicate corresponding means.

Figure 6. Plot-level wood density variation across forests types including: Lowland (Ltf = Lowland terra firme, Lfp = Lowland floodplain, Lbb = Lowland bamboo dominated forest; <500 m), submontane (SM: 500–1500 m), lower montane (LM: 1500–2500 m), upper montane (UP: 2500–3400 m) and tree line (TL: >3400 m) for (a) species mean WD including all arborescent life forms and (b) tree species. (c) Stem-weighted WD for all arborescent life forms and (d) tree stems. Box plots show 25% quartile, median, and 75% quartile of the distribution (horizontal lines). Forest types are defined based on Young (1992) and Pennington et al. (2004).

Figure 7. (a) Mean wood density variation for individual stems across DBH classes. Regression lines were computed using the mean averaged wood density across diameter classes for each forest type. Stars represent significant relationships. (b) Coefficient of variation (CV) of wood density across diameter classes—CV was calculated using the mean averaged wood density across diameter classes for each forest type. Color lines correspond to the same forest types for both (a) and (b).

Figure 8. Mean wood density and landslide stability (LS) as a function of elevation along the Andes-to-Amazon transect. LS was calculated as the inverted scale of landslide probability (1-landslide probability [$\%yr^{-1}$]) taken from Clark et al. (2015). Species mean wood density includes (a) all arborescent life forms and (b) trees only. Vertical dashed lines represent the cloud base in the gradient. Open circles represent mean species wood density and gray triangles landslide stability.

784 **Figure 1.**

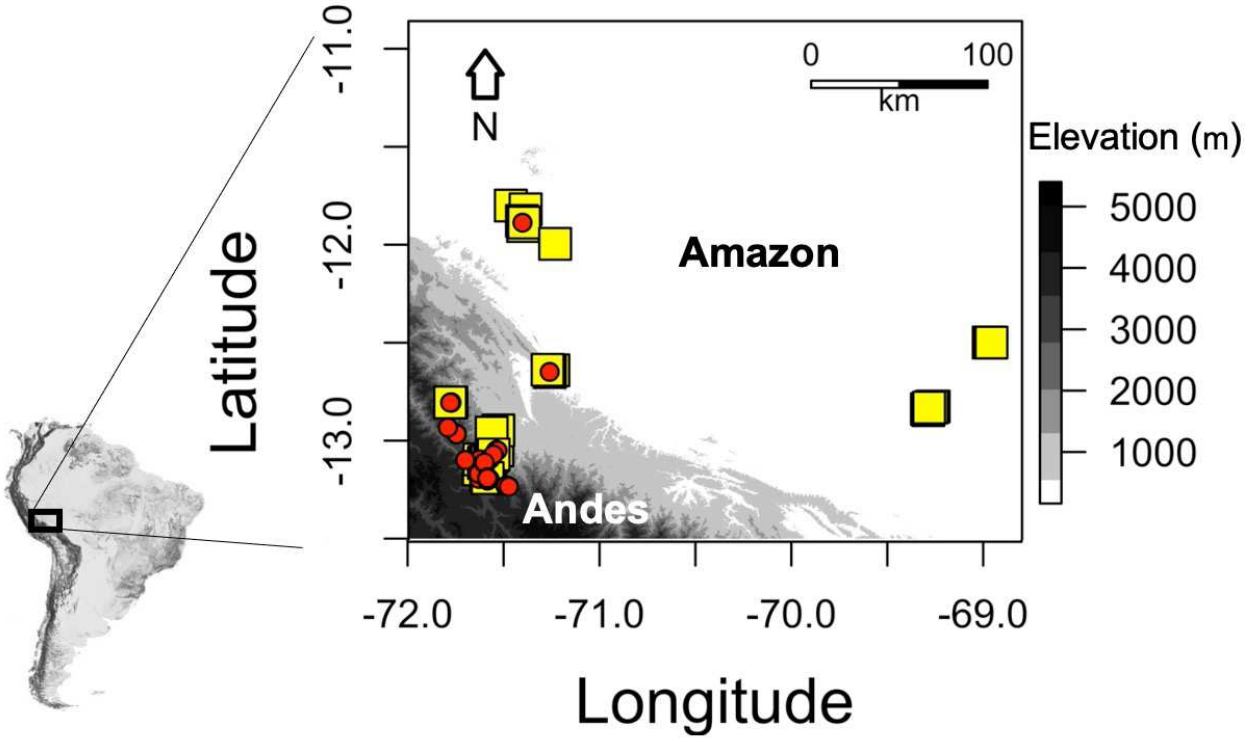
Latitude
-11.0
-12.0
-13.0
N
0
100
km
Amazon
Andes
Elevation (m)
5000
4000
3000
2000
1000
-72.0
-71.0
-70.0
-69.0
Longitude

785 **Figure 2.**

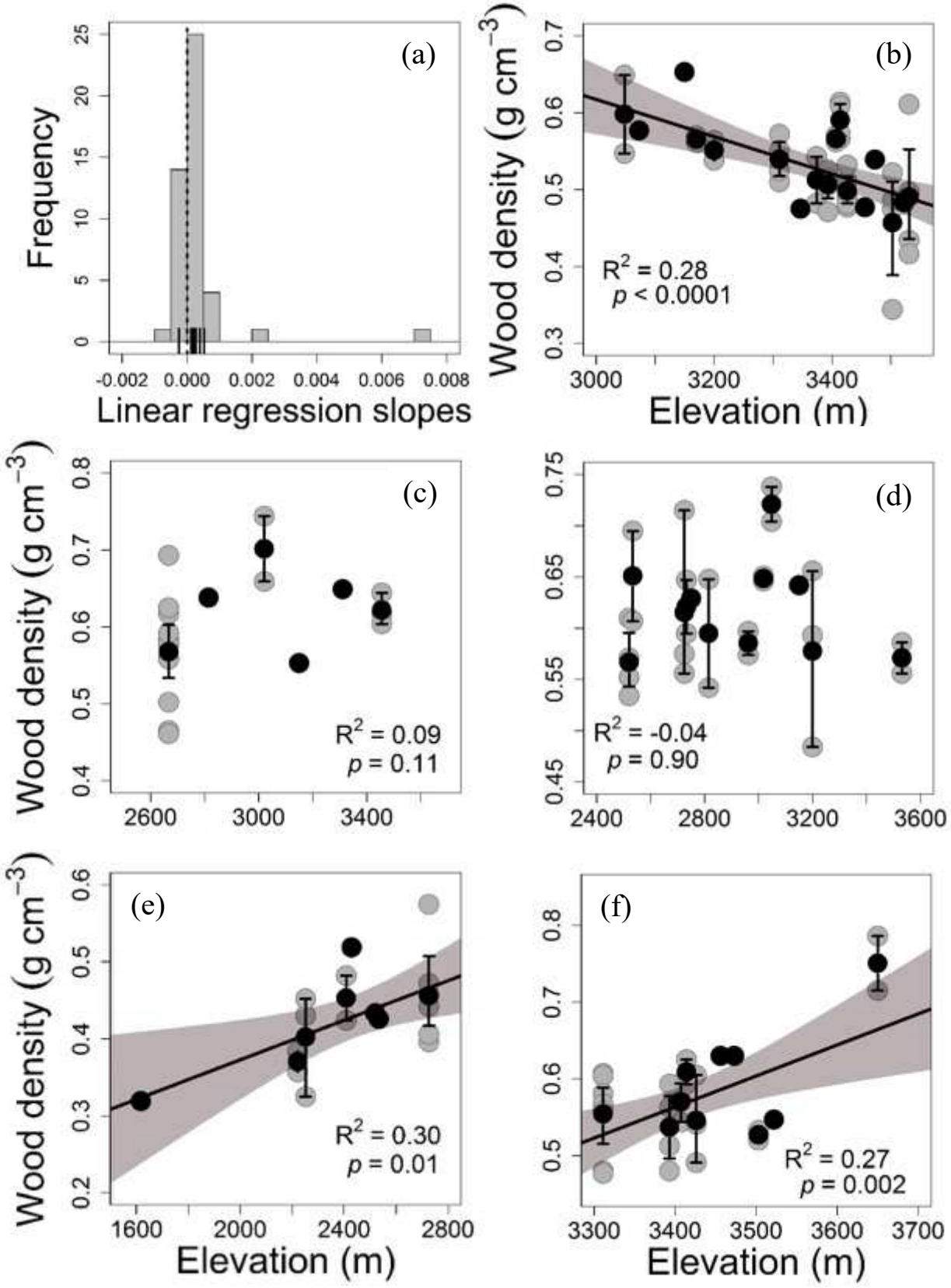
(a)
Frequency
Linear regression slopes
(b)
Wood density (g cm^{-3})
Elevation (m)
R^2 = 0.28
p < 0.0001
(c)
R^2 = 0.09
p = 0.11
(d)
R^2 = -0.04
p = 0.90
(e)
R^2 = 0.30
p = 0.01
(f)
R^2 = 0.27
p = 0.002

786 **Figure 3.**

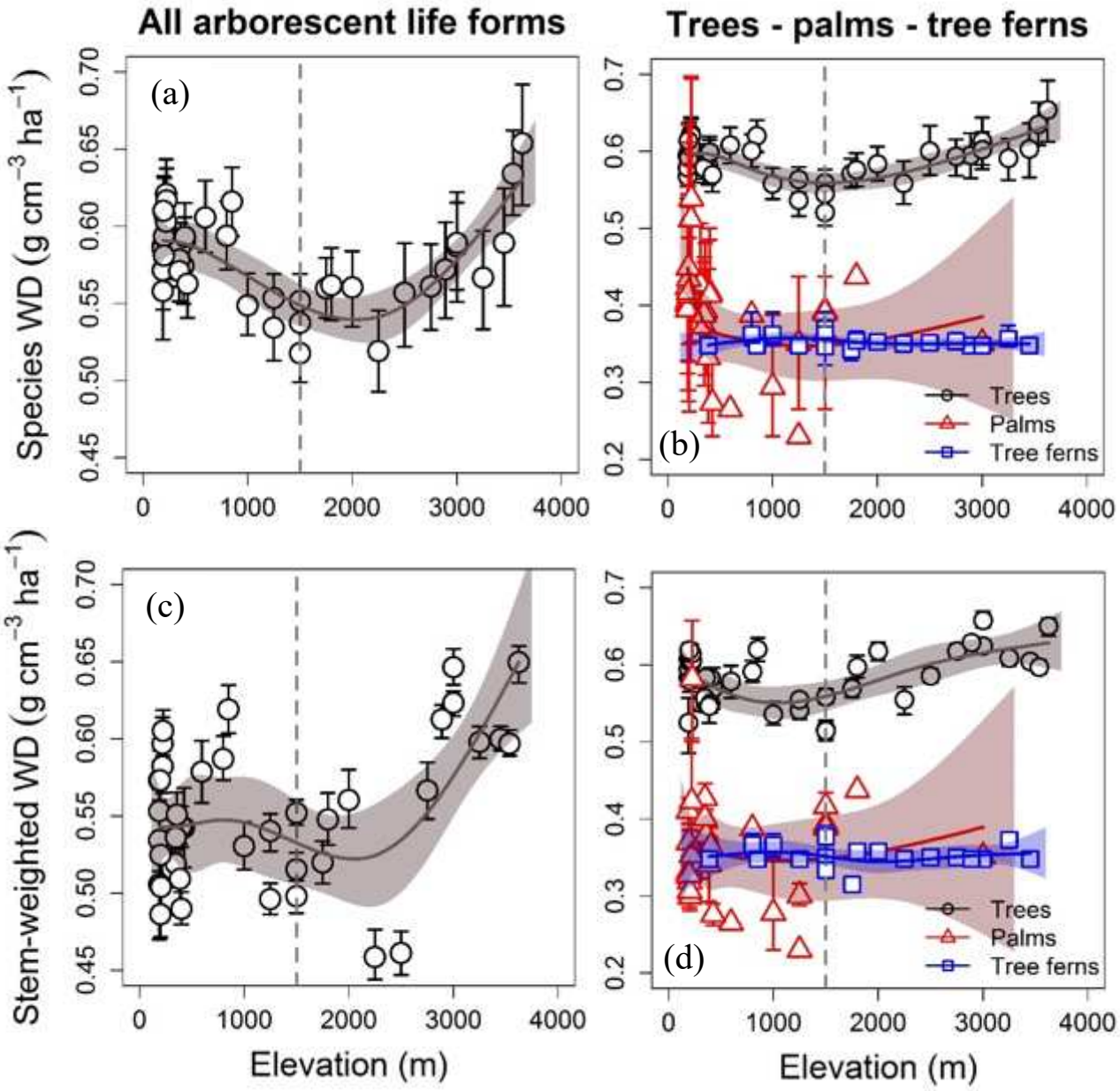
All arborescent life forms
Trees - palms - tree ferns
(a)
(b)
(c)
(d)
Species WD (g cm^{-3} ha^{-1})
Stem-weighted WD (g cm^{-3} ha^{-1})
Elevation (m)
Trees
Palms
Tree ferns

787 **Figure 4.**

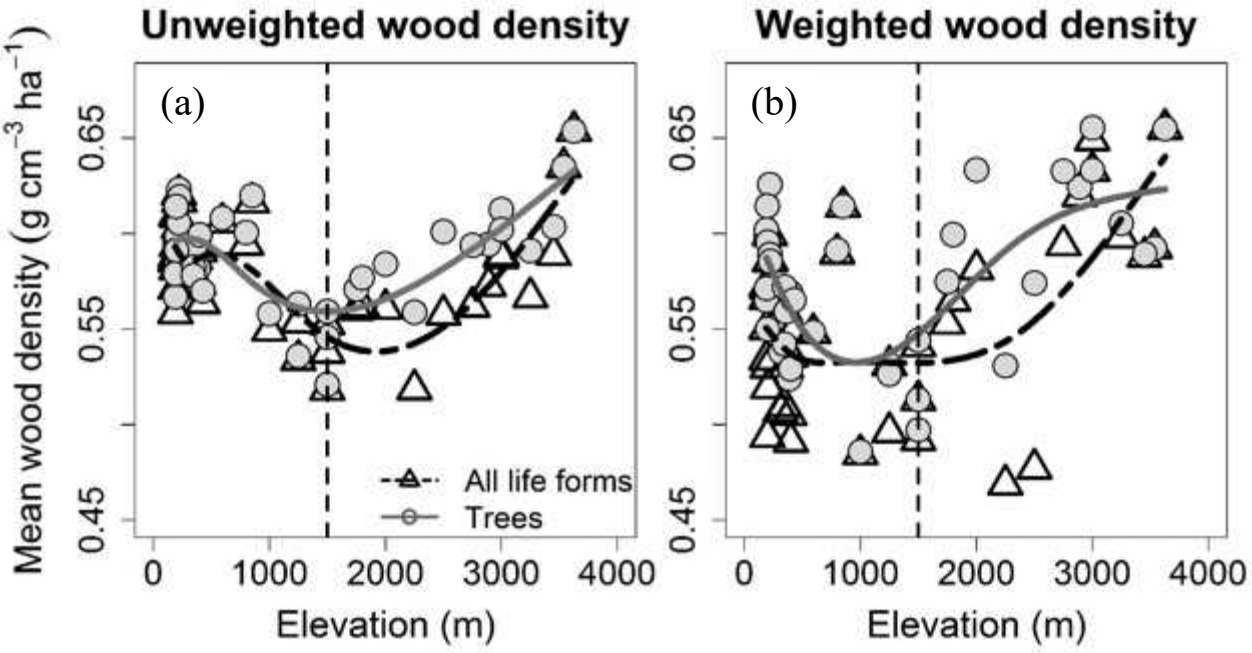
Unweighted wood density
Weighted wood density
(a)
(b)
Mean wood density (g cm^{-3} ha^{-1})
0.45
0.55
0.65
0
1000
2000
3000
4000
Elevation (m)
All life forms
Trees

788 **Figure 5.**

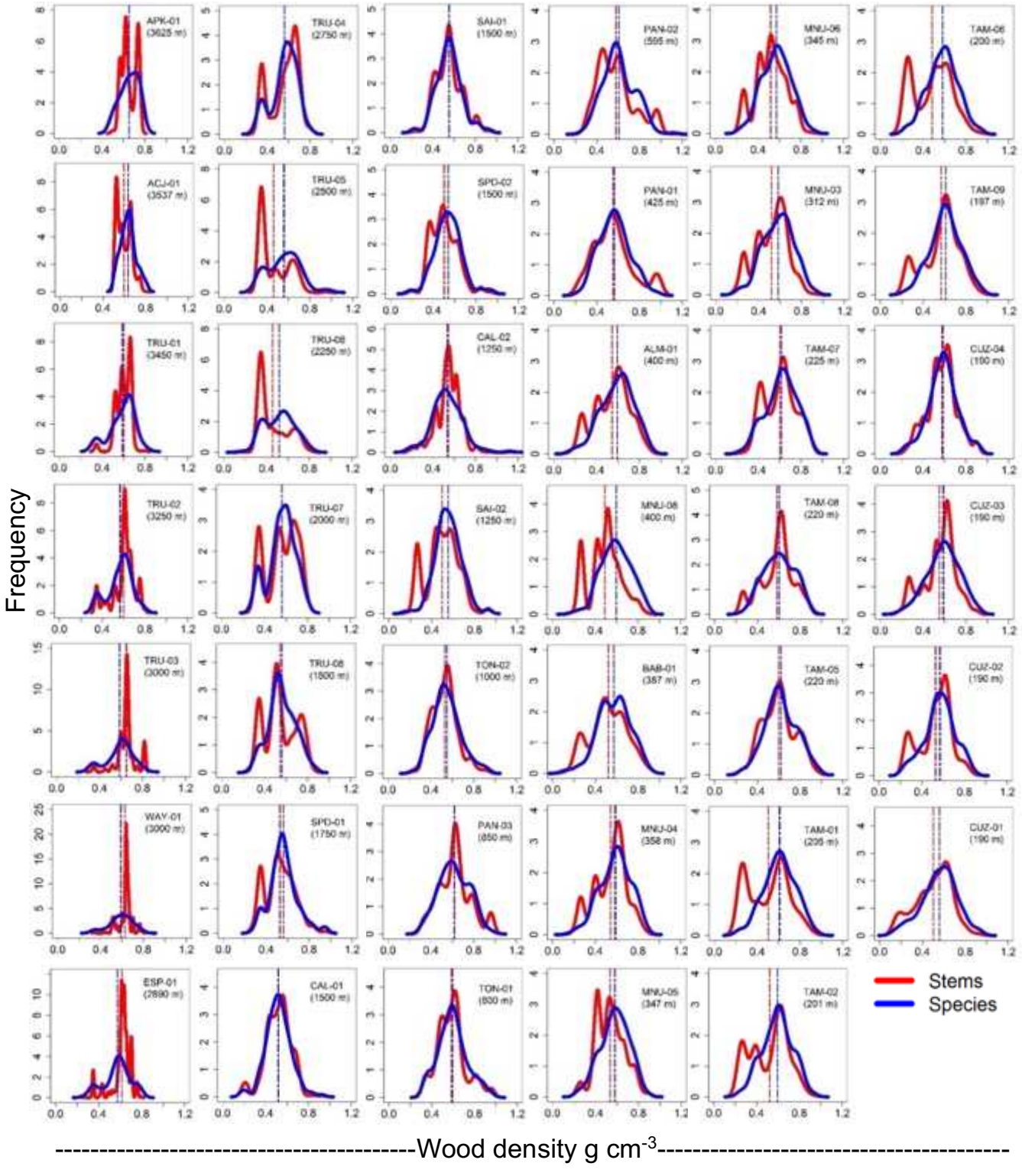

789 **Figure 6.**

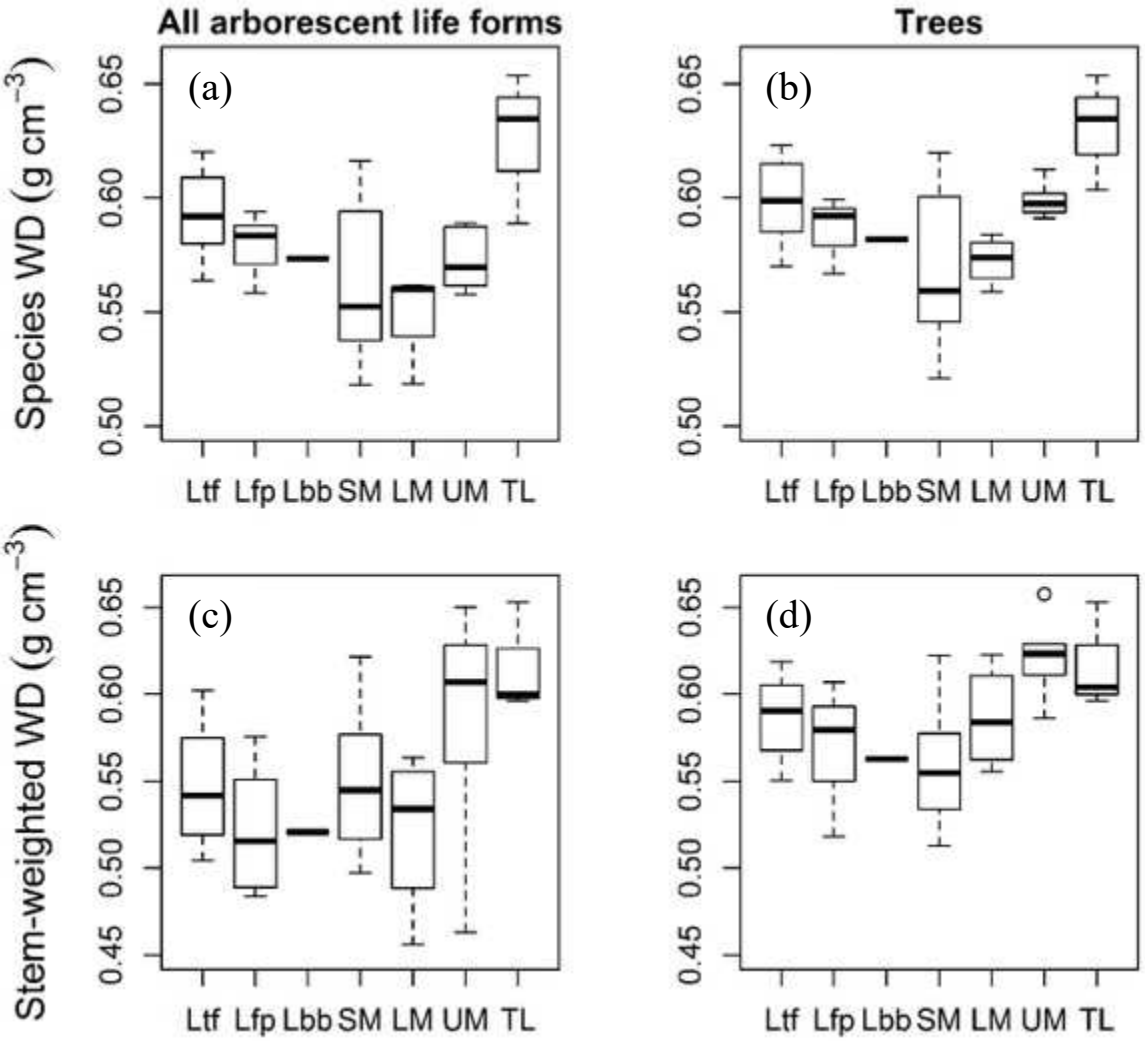
All arborescent life forms
Trees
(a)
(b)
(c)
(d)
Species WD (g cm^{-3})
Stem-weighted WD (g cm^{-3})
0.45
0.50
0.55
0.60
0.65
Ltf Lfp Lbb SM LM UM TL

790 **Figure 7.**

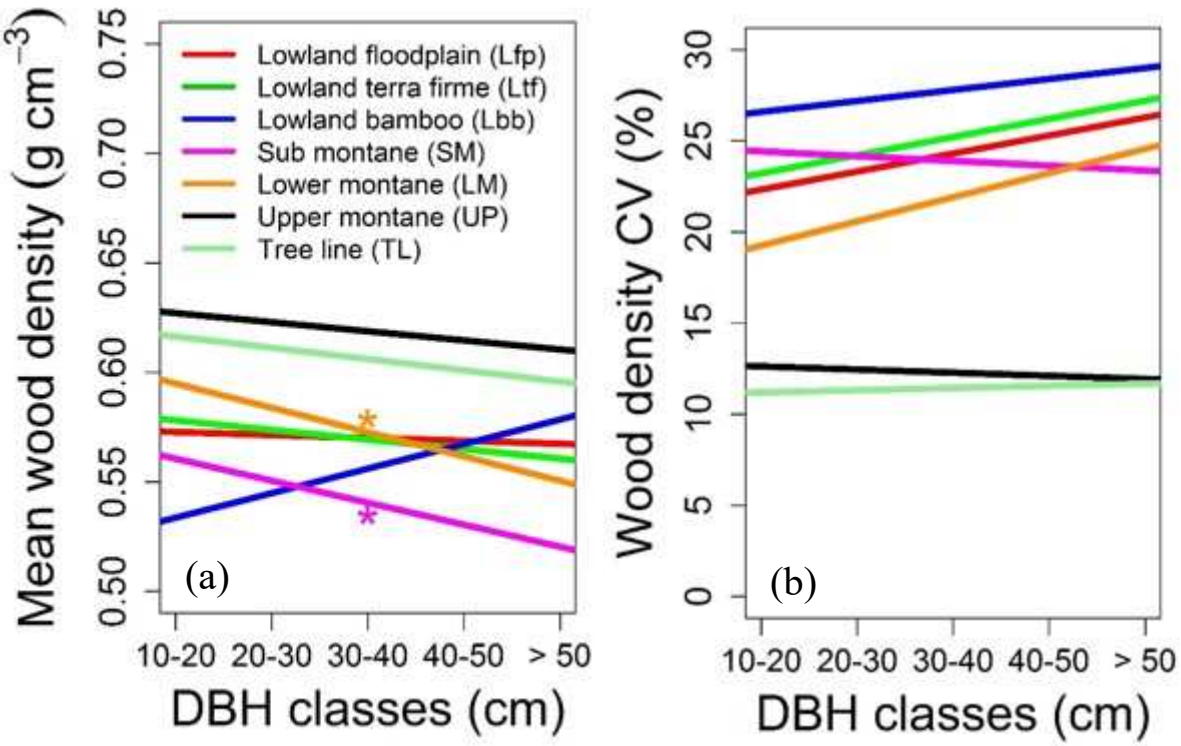
Mean wood density (g cm^{-3})
0.50
0.55
0.60
0.65
0.70
0.75
Lowland floodplain (Lfp)
Lowland terra firme (Ltf)
Lowland bamboo (Lbb)
Sub montane (SM)
Lower montane (LM)
Upper montane (UP)
Tree line (TL)
*
*
(a)
10-20
20-30
30-40
40-50
> 50
DBH classes (cm)
Wood density CV (%)
0
5
10
15
20
25
30
(b)
10-20
20-30
30-40
40-50
> 50
DBH classes (cm)

Figure 8.

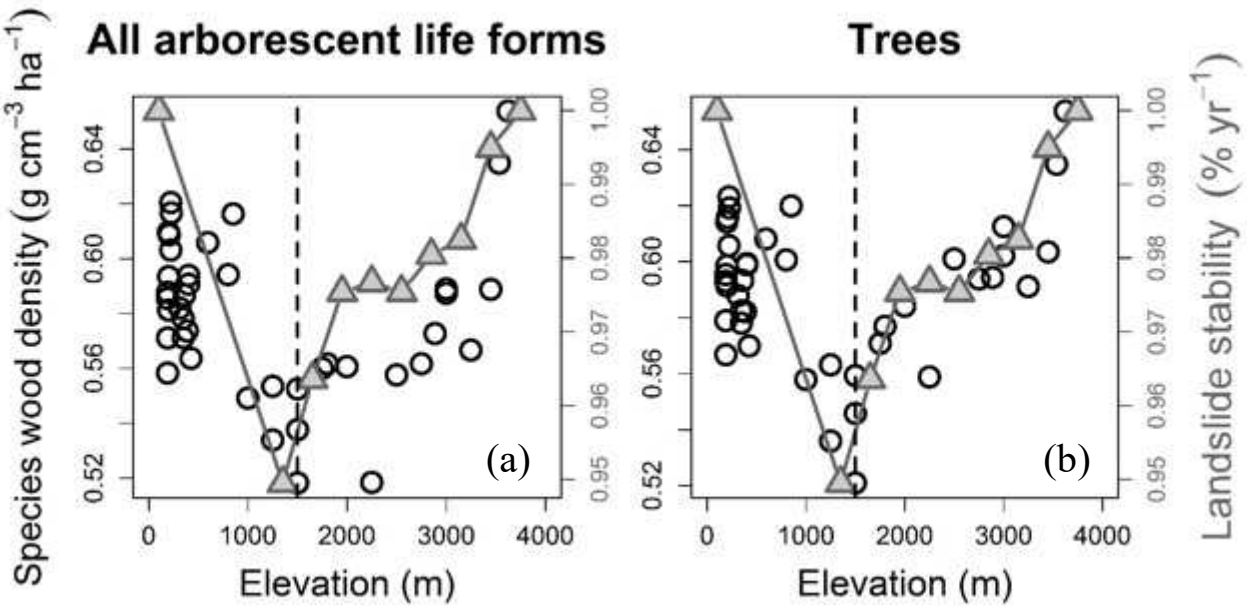
All arborescent life forms
Trees
Species wood density (g cm^{-3} ha^{-1})
Landslide stability (% yr^{-1})
Elevation (m)
Elevation (m)
(a)
(b)
0.52
0.56
0.60
0.64
0.95
0.96
0.97
0.98
0.99
1.00
0
1000
2000
3000
4000

Supporting Information

Article title: Wood density variation across an Andes-to-Amazon elevational gradient

Results

Across all elevations, the overall distribution of species mean Wood Density (WD) for all arborescent life forms and trees alone was symmetric and normal with a slight positive skewness and kurtosis (all life forms: Skewness = 0.07, kurtosis = 2.96; trees: Skewness = 0.09, kurtosis = 3.1). Likewise, the distribution of stem-weighted mean wood density for all arborescent life forms and for trees alone were symmetric and normal but were negatively skewed with positive kurtosis for both, all arborescent (skewness = -0.18, kurtosis = 2.70) and tree stems (skewness = -0.13, kurtosis = 3.53) (Fig. S2).

Plot-to-plot wood density distributions and their statistical moments varied across elevations. Species WD distributions shifted from a negative skew in the lowlands to a positive skew in the submontane forest and shifted again to a negative skew in the montane to tree line forest plots, with this pattern being similar for all arborescent life forms and trees only (Table S2). The montane and lowland plots showed a negative kurtosis, but we observed a positive kurtosis only in the submontane forest plots (Table S2). For stem WD distributions, we observed a marked increase in the right skew (right tail increasing) in plots with a high abundance of few species with low wood density values in the montane (e.g., TRU-05, TRU-06) and lowland forests plots (e.g., TAM-01,

828 MNU-08; Table S2). Kurtosis for stem WD distributions for all arborescent life forms and only
829 trees varied along the gradient, with the predominance of negative kurtosis in the lowland forests
830 (Table S2).

Table S1. Site description and mean wood density values for 41 (47.5 ha) forest plots across the Andes-to-Amazon elevational gradient.

Plot	Elevation (m)	Size (ha)	Forest type	Basal area (m^2 ha^{-1})				Mean wood density (g cm^{-3})											
								Species				Stems				Basal area			
				All life forms	Trees	Palms	Tree ferns	All life forms	Trees	Palms	Tree ferns	All life forms	Trees	Palms	Tree ferns	All life forms	Trees	Palms	Tree ferns
APK-01	3625	1	Tree line	21.2	21.2	-	-	0.654	0.654	-	-	0.653	0.653	-	-	0.655	0.655	-	-
ACJ-01	3537	1	Tree line	37.3	37.3	-	-	0.635	0.635	-	-	0.596	0.596	-	-	0.592	0.592	-	-
TRU-01	3450	1	Tree line	28.6	28.4	-	0.2	0.589	0.603	-	0.348	0.600	0.604	-	0.348	0.588	0.589	-	0.348
TRU-02	3250	1	Upper montane	31.2	30.2	-	1.0	0.567	0.591	-	0.357	0.600	0.611	-	0.370	0.598	0.605	-	0.373
TRU-03	3000	1	Upper montane	20.5	20.0	0.0	0.4	0.587	0.612	0.351	0.348	0.650	0.658	0.351	0.348	0.649	0.655	0.351	0.348
WAY-01	3000	1	Upper montane	34.3	34.3	-	0.0	0.589	0.602	-	0.348	0.628	0.629	-	0.348	0.633	0.633	-	0.348
ESP-01	2890	1	Upper montane	28.2	27.7	-	0.5	0.573	0.594	-	0.348	0.614	0.628	-	0.348	0.620	0.624	-	0.348
TRU-04	2750	1	Upper montane	34.7	29.9	-	4.7	0.562	0.594	-	0.353	0.561	0.618	-	0.350	0.594	0.633	-	0.349
TRU-05	2500	1	Upper montane	43.5	24.6	-	18.8	0.558	0.601	-	0.351	0.463	0.586	-	0.350	0.477	0.574	-	0.350
TRU-06	2250	1	Lower montane	37.0	24.4	-	12.6	0.518	0.559	-	0.350	0.456	0.556	-	0.348	0.469	0.531	-	0.348
TRU-07	2000	1	Lower montane	21.0	17.0	-	4.0	0.561	0.584	-	0.353	0.564	0.623	-	0.359	0.581	0.633	-	0.359
TRU-08	1800	1	Lower montane	29.6	25.4	0.1	4.2	0.562	0.577	0.437	0.354	0.547	0.599	0.437	0.358	0.565	0.599	0.437	0.358
SPD-01	1750	1	Lower montane	36.5	33.5	-	3.1	0.560	0.571	-	0.343	0.521	0.569	-	0.316	0.553	0.575	-	0.313

Plot	Elevation (m)	Size (ha)	Forest type	Basal area (m^2 ha^{-1})				Mean wood density (g cm^{-3})											
								Species				Stems				Basal area			
				All life forms	Trees	Palms	Tree ferns	All life forms	Trees	Palms	Tree ferns	All life forms	Trees	Palms	Tree ferns	All life forms	Trees	Palms	Tree ferns
CAL-01	1500	1	Submontane	30.8	30.7	0.0	0.0	0.518	0.521	0.393	0.369	0.517	0.517	0.393	0.377	0.513	0.513	0.393	0.376
SAI-01	1500	1	Submontane	41.2	40.4	0.7	0.2	0.552	0.559	0.363	0.362	0.553	0.559	0.414	0.353	0.541	0.544	0.412	0.351
SPD-02	1500	1	Submontane	30.4	29.4	0.1	0.9	0.538	0.546	0.390	0.347	0.499	0.513	0.388	0.332	0.492	0.497	0.388	0.333
CAL-02	1250	1	Submontane	37.0	36.9	0.0	-	0.534	0.536	0.230	-	0.545	0.545	0.230	-	0.531	0.531	0.230	-
SAI-02	1250	1	Submontane	42.2	36.3	5.7	0.2	0.553	0.563	0.351	0.348	0.497	0.555	0.310	0.348	0.496	0.526	0.308	0.348
TON-02	1000	1	Submontane	31.3	31.1	0.1	0.1	0.549	0.558	0.294	0.362	0.529	0.534	0.278	0.364	0.484	0.486	0.257	0.367
PAN-03	850	1	Submontane	24.2	24.2	-	0.0	0.616	0.620	-	0.348	0.622	0.622	-	0.348	0.614	0.614	-	0.348
TON-01	800	1	Submontane	26.5	26.3	0.0	0.2	0.594	0.601	0.388	0.362	0.586	0.589	0.388	0.369	0.590	0.591	0.388	0.370
PAN-02	595	1	Submontane	27.7	27.7	0.0	-	0.606	0.608	0.265	-	0.577	0.577	0.265	-	0.548	0.548	0.265	-
PAN-01	425	1	Lowland (TF)	27.3	25.8	1.4	-	0.564	0.570	0.274	-	0.551	0.577	0.271	-	0.550	0.565	0.271	-
ALM-01	400	2	Lowland (TF)	31.2	26.9	4.3	-	0.591	0.599	0.419	-	0.542	0.580	0.347	-	0.536	0.569	0.327	-
MNU-08	400	2	Lowland (FP)	41.8	33.9	7.9	-	0.594	0.599	0.413	-	0.489	0.550	0.364	-	0.491	0.529	0.328	-
BAB-01	387	1	Lowland (BB)	29.3	26.9	2.4	0.0	0.574	0.582	0.332	0.348	0.521	0.563	0.335	0.348	0.505	0.524	0.289	0.348
MNU-04	358	2	Lowland (TF)	28.2	24.3	3.9	-	0.587	0.593	0.392	-	0.541	0.580	0.365	-	0.530	0.559	0.350	-
MNU-05	347	2.25	Lowland (TF)	30.7	28.6	2.1	-	0.578	0.582	0.373	-	0.536	0.551	0.430	-	0.559	0.572	0.391	-
MNU-06	345	2.25	Lowland (TF)	32.3	27.0	5.3	-	0.571	0.578	0.388	-	0.517	0.559	0.383	-	0.510	0.542	0.350	-

Plot	Elevation (m)	Size (ha)	Forest type	Basal area (m^2 ha^{-1})				Mean wood density (g cm^{-3})											
								Species				Stems				Basal area			
				All life forms	Trees	Palms	Tree ferns	All life forms	Trees	Palms	Tree ferns	All life forms	Trees	Palms	Tree ferns	All life forms	Trees	Palms	Tree ferns
MNU-03	312	2	Lowland (TF)	30.3	26.1	4.2	-	0.582	0.588	0.427	-	0.518	0.552	0.340	-	0.507	0.538	0.315	-
TAM-07	225	1	Lowland (TF)	25.5	25.2	0.4	-	0.617	0.619	0.539	-	0.602	0.602	0.588	-	0.586	0.585	0.609	-
TAM-05	220	1	Lowland (TF)	27.6	27.1	0.5	-	0.620	0.623	0.512	-	0.600	0.606	0.436	-	0.585	0.589	0.406	-
TAM-08	220	1	Lowland (TF)	22.2	20.3	2.0	-	0.603	0.606	0.512	-	0.583	0.614	0.360	-	0.599	0.626	0.328	-
TAM-01	205	1	Lowland (TF)	28.8	22.0	6.8	-	0.609	0.616	0.418	-	0.504	0.601	0.292	-	0.519	0.595	0.275	-
TAM-02	201	1	Lowland (TF)	28.1	22.0	6.1	-	0.593	0.599	0.434	-	0.520	0.604	0.315	-	0.530	0.595	0.293	-
TAM-06	200	1	Lowland (FP)	37.6	29.4	8.2	-	0.581	0.591	0.418	-	0.484	0.574	0.292	-	0.493	0.550	0.290	-
TAM-09	197	1	Lowland (TF)	23.3	20.3	3.0	-	0.610	0.614	0.455	-	0.567	0.619	0.298	-	0.571	0.614	0.283	-
CUZ-01	190	1	Lowland (FP)	27.2	25.5	1.7	-	0.558	0.567	0.403	-	0.502	0.518	0.358	-	0.550	0.565	0.333	-
CUZ-02	190	1	Lowland (FP)	27.9	24.0	3.9	-	0.571	0.579	0.405	-	0.529	0.585	0.315	-	0.534	0.571	0.305	-
CUZ-03	190	1	Lowland (FP)	27.7	24.5	3.2	-	0.588	0.595	0.432	-	0.551	0.593	0.327	-	0.566	0.598	0.314	-
CUZ-04	190	1	Lowland (FP)	28.1	24.4	3.6	-	0.585	0.593	0.405	-	0.576	0.607	0.409	-	0.572	0.602	0.372	-

833

834

Table S2. Statistical moments of mean wood density (g cm^{-3}) distribution on species and stem levels for 41 permanent plots across the Andes-to-Amazon elevational gradient.

Plot	Elevation (m)	Species WD								Stem-weighted WD							
		All arborescent life forms				Trees				All arborescent life forms				Trees			
		mean	sd	skewness	kurtosis	mean	sd	skewness	kurtosis	mean	sd	skewness	kurtosis	mean	sd	skewness	kurtosis
APK-01	3625	0.654	0.084	-0.415	-0.984	0.654	0.084	-0.415	-0.984	0.653	0.067	0.085	-1.355	0.653	0.067	0.085	-1.355
ACJ-01	3537	0.635	0.071	0.360	-0.250	0.635	0.071	0.360	-0.250	0.596	0.065	0.451	-0.862	0.596	0.065	0.451	-0.862
TRU-01	3450	0.589	0.115	-0.798	0.065	0.603	0.101	-0.835	0.756	0.600	0.069	-1.114	2.390	0.604	0.061	-0.676	1.195
TRU-02	3250	0.567	0.113	-0.480	-0.267	0.591	0.091	-0.340	0.507	0.600	0.103	-0.876	0.529	0.611	0.091	-0.878	1.211
TRU-03	3000	0.587	0.122	-0.618	-0.061	0.612	0.098	-0.529	1.002	0.650	0.088	-0.596	2.926	0.658	0.074	0.368	1.683
WAY-01	3000	0.589	0.107	-0.515	-0.022	0.602	0.093	-0.286	-0.015	0.628	0.066	-1.046	3.475	0.629	0.065	-0.944	3.229
ESP-01	2890	0.573	0.125	-0.424	-0.253	0.594	0.108	-0.444	0.621	0.614	0.089	-1.591	2.815	0.628	0.066	-1.238	3.756
TRU-04	2750	0.562	0.117	-0.576	-0.328	0.594	0.090	-0.607	1.382	0.561	0.130	-0.566	-0.969	0.618	0.078	-0.546	0.386
TRU-05	2500	0.558	0.146	0.220	-0.166	0.601	0.122	0.385	0.952	0.463	0.136	0.728	-0.772	0.586	0.098	0.056	0.195
TRU-06	2250	0.518	0.136	0.014	-0.787	0.559	0.120	-0.348	0.336	0.456	0.137	0.807	-0.768	0.556	0.124	-0.228	-0.699
TRU-07	2000	0.561	0.123	-0.401	-0.379	0.584	0.106	-0.492	0.619	0.564	0.139	-0.330	-1.128	0.623	0.096	-0.496	0.148
TRU-08	1800	0.562	0.123	0.105	-0.305	0.577	0.114	0.169	-0.040	0.547	0.143	0.189	-1.057	0.599	0.116	0.244	-1.014
SPD-01	1750	0.560	0.129	0.553	0.856	0.571	0.122	0.704	1.180	0.521	0.144	0.086	-0.398	0.569	0.115	0.255	0.775
CAL-01	1500	0.518	0.118	0.160	1.152	0.521	0.118	0.131	1.251	0.517	0.118	-0.359	0.854	0.517	0.118	-0.375	0.895
SAI-01	1500	0.552	0.119	0.335	0.950	0.559	0.115	0.410	1.160	0.553	0.119	0.448	0.111	0.559	0.117	0.472	0.143

Plot	Elevation (m)	Species WD								Stem-weighted WD							
		All arborescent life forms				Trees				All arborescent life forms				Trees			
		mean	sd	skewness	kurtosis	mean	sd	skewness	kurtosis	mean	sd	skewness	kurtosis	mean	sd	skewness	kurtosis
SPD-02	1500	0.538	0.127	0.276	1.167	0.546	0.123	0.268	1.515	0.499	0.124	0.535	0.649	0.513	0.119	0.538	0.949
CAL-02	1250	0.534	0.140	0.415	1.792	0.536	0.138	0.461	1.889	0.545	0.111	-0.285	1.676	0.545	0.110	-0.271	1.686
SAI-02	1250	0.553	0.121	0.050	0.784	0.563	0.115	0.115	1.211	0.497	0.147	0.020	-0.217	0.555	0.112	0.354	1.289
TON-02	1000	0.549	0.132	0.464	0.258	0.558	0.126	0.606	0.283	0.529	0.118	0.514	0.523	0.534	0.115	0.605	0.563
PAN-03	850	0.616	0.140	0.057	-0.620	0.620	0.138	0.082	-0.610	0.622	0.150	0.310	-0.085	0.622	0.150	0.316	-0.075
TON-01	800	0.594	0.135	0.358	-0.037	0.601	0.131	0.402	0.051	0.586	0.134	0.591	0.472	0.589	0.132	0.621	0.543
PAN-02	595	0.606	0.148	0.371	0.005	0.608	0.146	0.429	-0.020	0.577	0.171	0.763	-0.053	0.577	0.171	0.770	-0.053
PAN-01	425	0.564	0.143	0.265	-0.226	0.570	0.138	0.381	-0.271	0.551	0.182	0.625	0.041	0.577	0.168	0.849	0.150
ALM-01	400	0.591	0.153	-0.349	-0.220	0.599	0.148	-0.355	-0.105	0.542	0.164	-0.232	-0.690	0.580	0.143	-0.329	-0.106
MNU-08	400	0.594	0.139	-0.114	-0.294	0.599	0.136	-0.116	-0.261	0.489	0.147	0.061	-0.438	0.550	0.120	0.274	0.079
BAB-01	387	0.574	0.151	-0.285	0.007	0.582	0.146	-0.280	0.181	0.521	0.168	-0.062	-0.650	0.563	0.149	-0.127	-0.168
MNU-04	358	0.587	0.145	-0.303	-0.290	0.593	0.140	-0.283	-0.253	0.541	0.150	-0.348	-0.545	0.580	0.128	-0.479	0.197
MNU-05	347	0.578	0.134	-0.237	-0.354	0.582	0.132	-0.232	-0.316	0.536	0.131	0.176	-0.230	0.551	0.128	0.208	-0.390
MNU-06	345	0.571	0.135	-0.045	-0.348	0.578	0.132	-0.042	-0.287	0.517	0.140	-0.086	-0.482	0.559	0.121	0.004	-0.355
MNU-03	312	0.582	0.144	-0.153	-0.274	0.588	0.142	-0.155	-0.232	0.518	0.149	-0.251	-0.579	0.552	0.131	-0.332	0.073
TAM-07	225	0.617	0.145	-0.281	-0.492	0.619	0.142	-0.205	-0.605	0.602	0.146	0.024	-0.893	0.602	0.145	0.069	-0.930
TAM-05	220	0.620	0.148	0.079	-0.319	0.623	0.145	0.145	-0.356	0.600	0.149	0.127	-0.604	0.606	0.144	0.227	-0.676
TAM-08	220	0.603	0.142	-0.054	-0.822	0.606	0.139	0.009	-0.889	0.583	0.151	-0.372	-0.287	0.614	0.123	-0.002	-0.261

Plot	Elevation (m)	Species WD								Stem-weighted WD							
		All arborescent life forms				Trees				All arborescent life forms				Trees			
		mean	sd	skewness	kurtosis	mean	sd	skewness	kurtosis	mean	sd	skewness	kurtosis	mean	sd	skewness	kurtosis
TAM-01	205	0.609	0.147	-0.152	-0.271	0.616	0.140	0.026	-0.474	0.504	0.187	0.008	-1.180	0.601	0.131	-0.111	-0.039
TAM-02	201	0.593	0.142	-0.110	-0.367	0.599	0.137	-0.010	-0.424	0.520	0.174	-0.147	-1.109	0.604	0.123	-0.346	0.112
TAM-06	200	0.581	0.143	-0.051	-0.171	0.591	0.138	-0.023	-0.102	0.484	0.175	-0.012	-1.072	0.574	0.125	-0.150	0.275
TAM-09	197	0.610	0.144	-0.088	-0.205	0.614	0.139	0.036	-0.315	0.567	0.167	-0.427	-0.530	0.619	0.122	-0.119	0.032
CUZ-01	190	0.558	0.164	-0.291	-0.007	0.567	0.160	-0.337	0.227	0.502	0.169	-0.378	-0.472	0.518	0.168	-0.594	-0.125
CUZ-02	190	0.571	0.143	-0.208	-0.162	0.579	0.137	-0.151	-0.076	0.529	0.149	-0.414	-0.542	0.585	0.105	-0.245	0.987
CUZ-03	190	0.588	0.151	-0.238	-0.243	0.595	0.147	-0.256	-0.081	0.551	0.150	-0.485	-0.249	0.593	0.118	-0.505	1.287
CUZ-04	190	0.585	0.137	-0.076	0.264	0.593	0.130	0.054	0.313	0.576	0.136	-0.027	-0.021	0.607	0.118	0.119	0.424

837

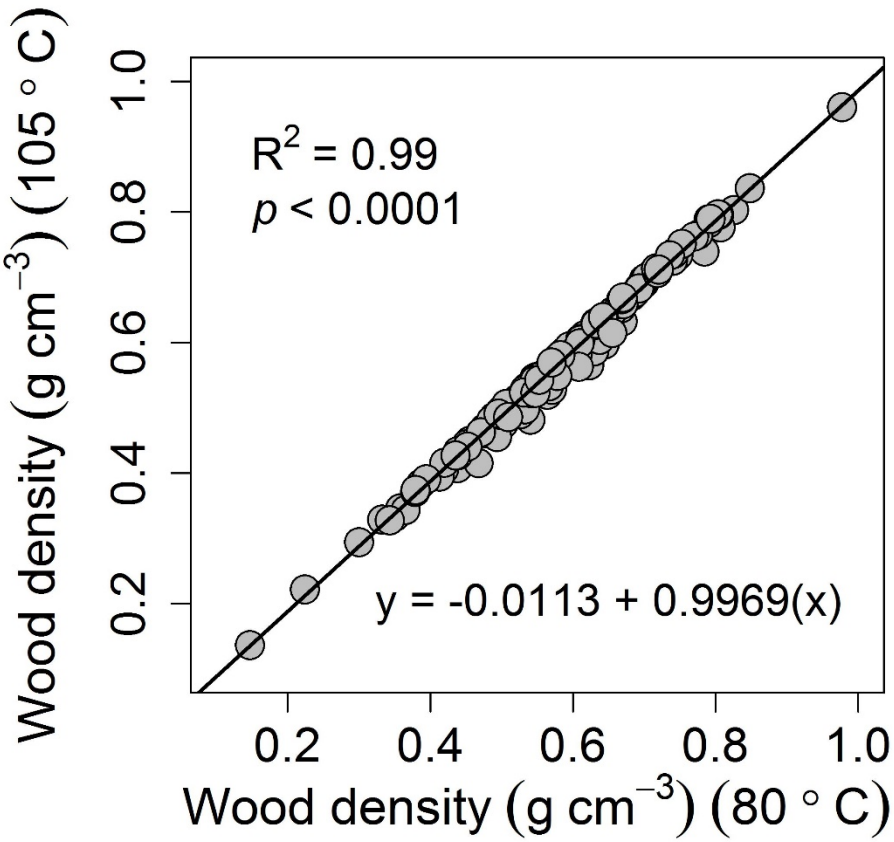

Fig. S1. The effect of drying temperature on basic wood specific gravity (wood density) values is shown by the relationship between wood density values dried at ~80 ° C and 105 ° C oven temperatures (n = 145). The equation y = -0.0113 + 0.9969(x) was used to calibrate all wood density values obtained at the ~80 ° C oven temperature.

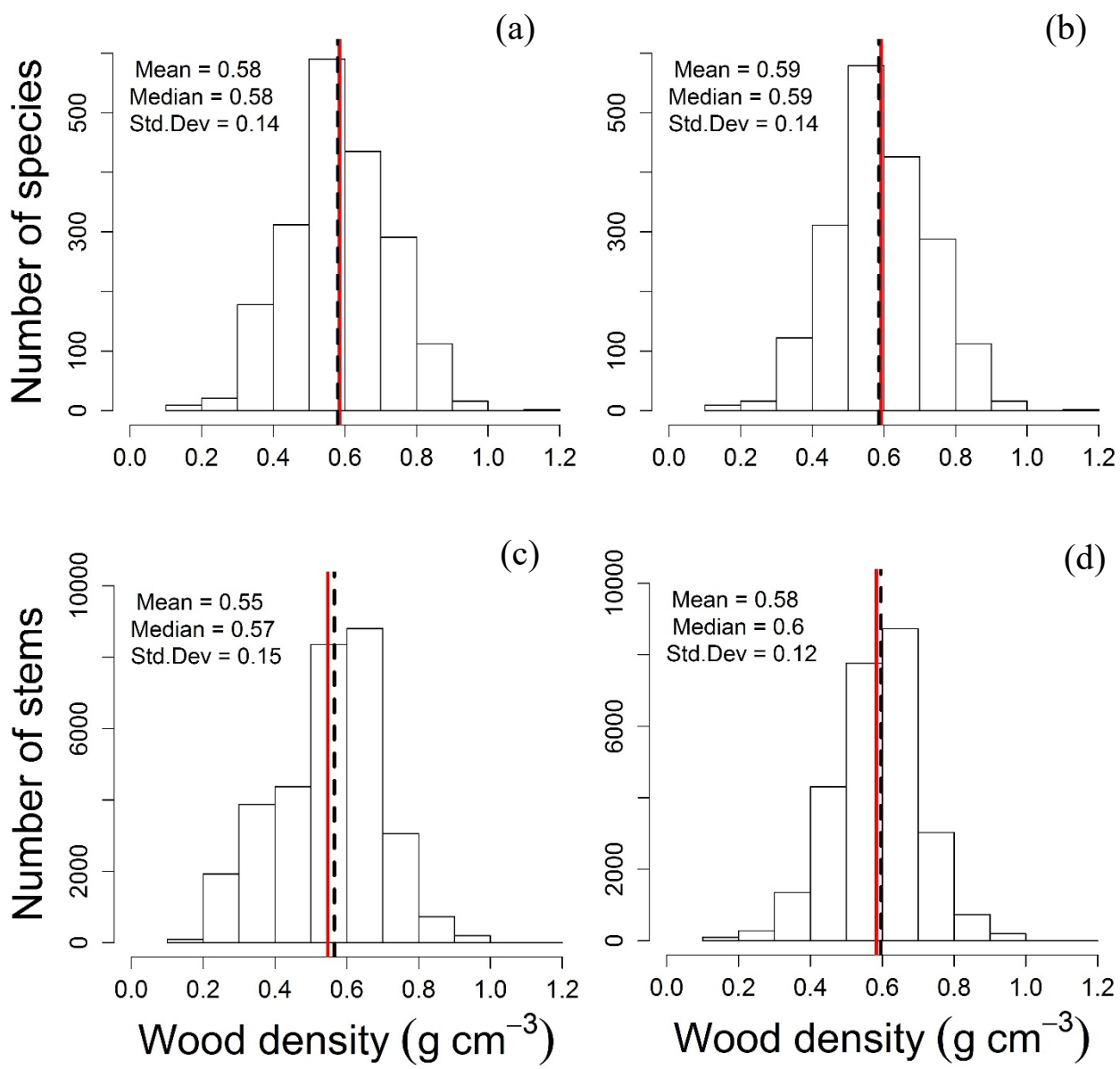

Fig. S2. Overall wood density distribution along the Andes-to-Amazon elevational gradient for species including (a) all arborescent life forms and (b) tree species. Mean wood density for all stems (c) including all arborescent life forms and (d) tree stems. Solid red vertical lines indicate the means and dashed black lines indicate the medians.

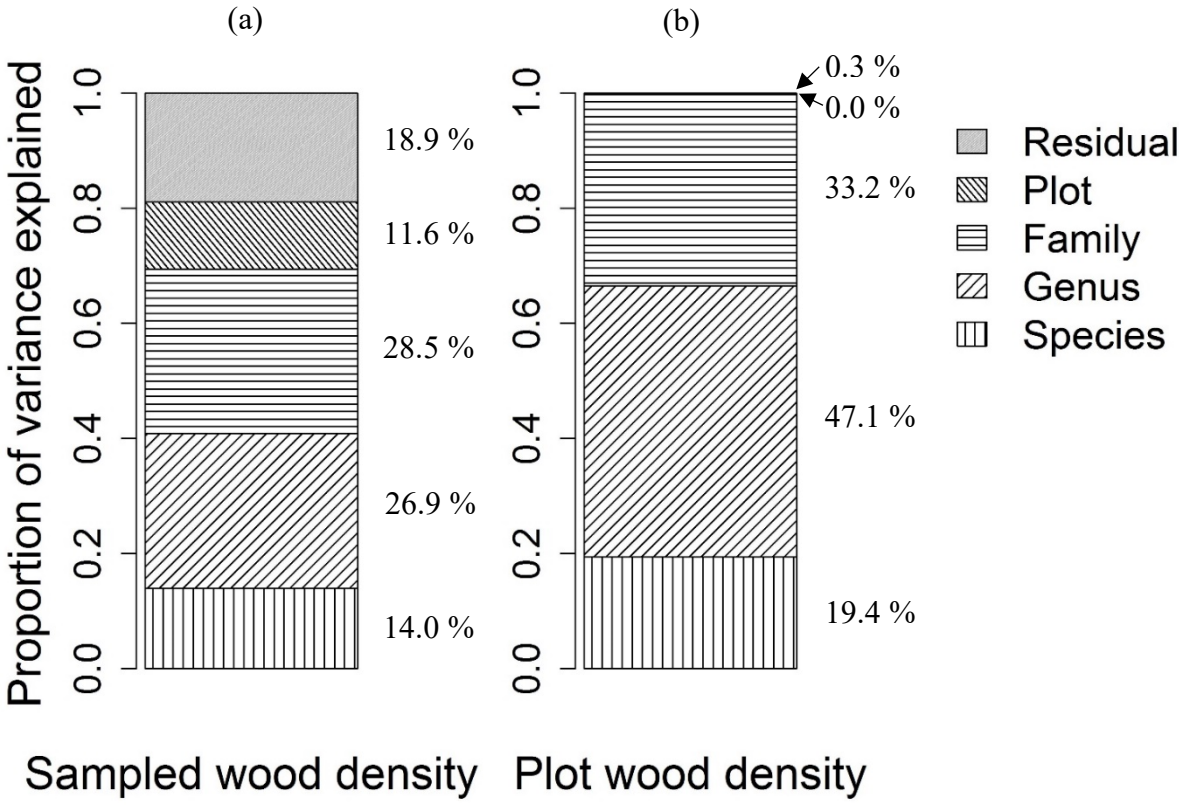

Fig. S3. Variance partitioning of wood density across phylogenetic levels and environment (plot level) for (a) field core-sampled and (b) plot level along the Andes-to-Amazon elevational gradient.

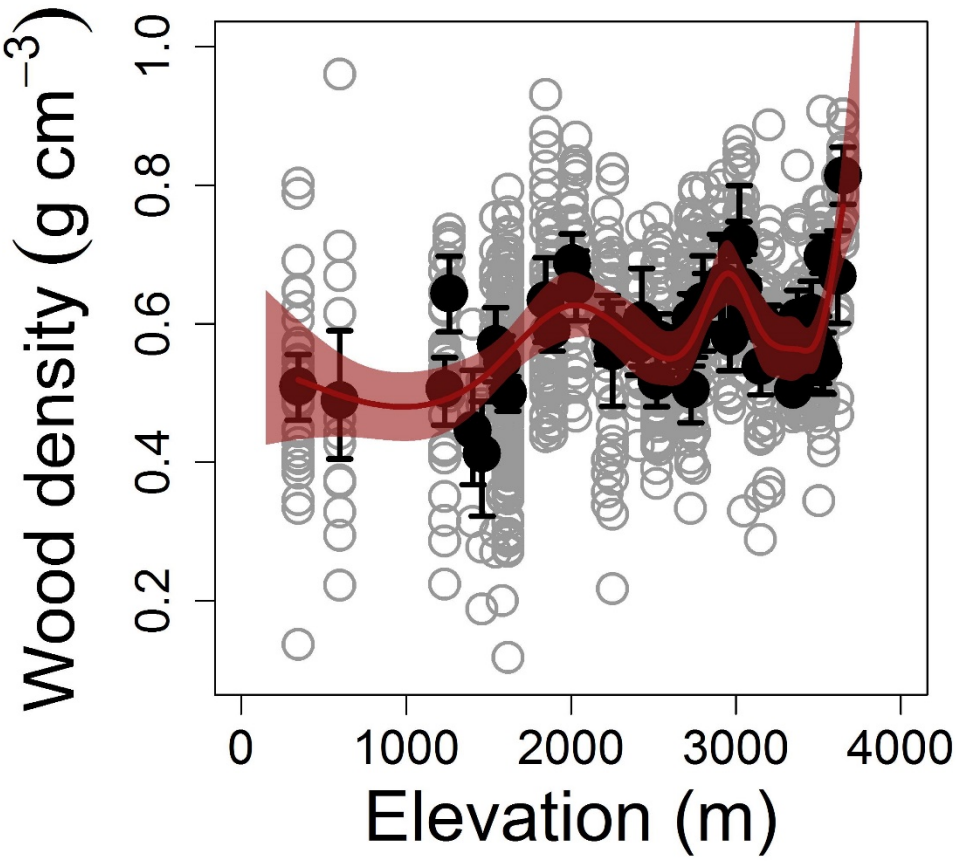

Fig. S4. Sampled wood density along an Andes-to-Amazon elevational gradient. Gray open circles represent stem core samples across elevation (n = 892), and black solid circles represent the mean wood density among samples at each sampled site (n = 51). The red solid line is the generalized additive model (GAM) fit using a smoothing function with 95% confidence limits. Error bars depict bootstrapped 95% confidence intervals.

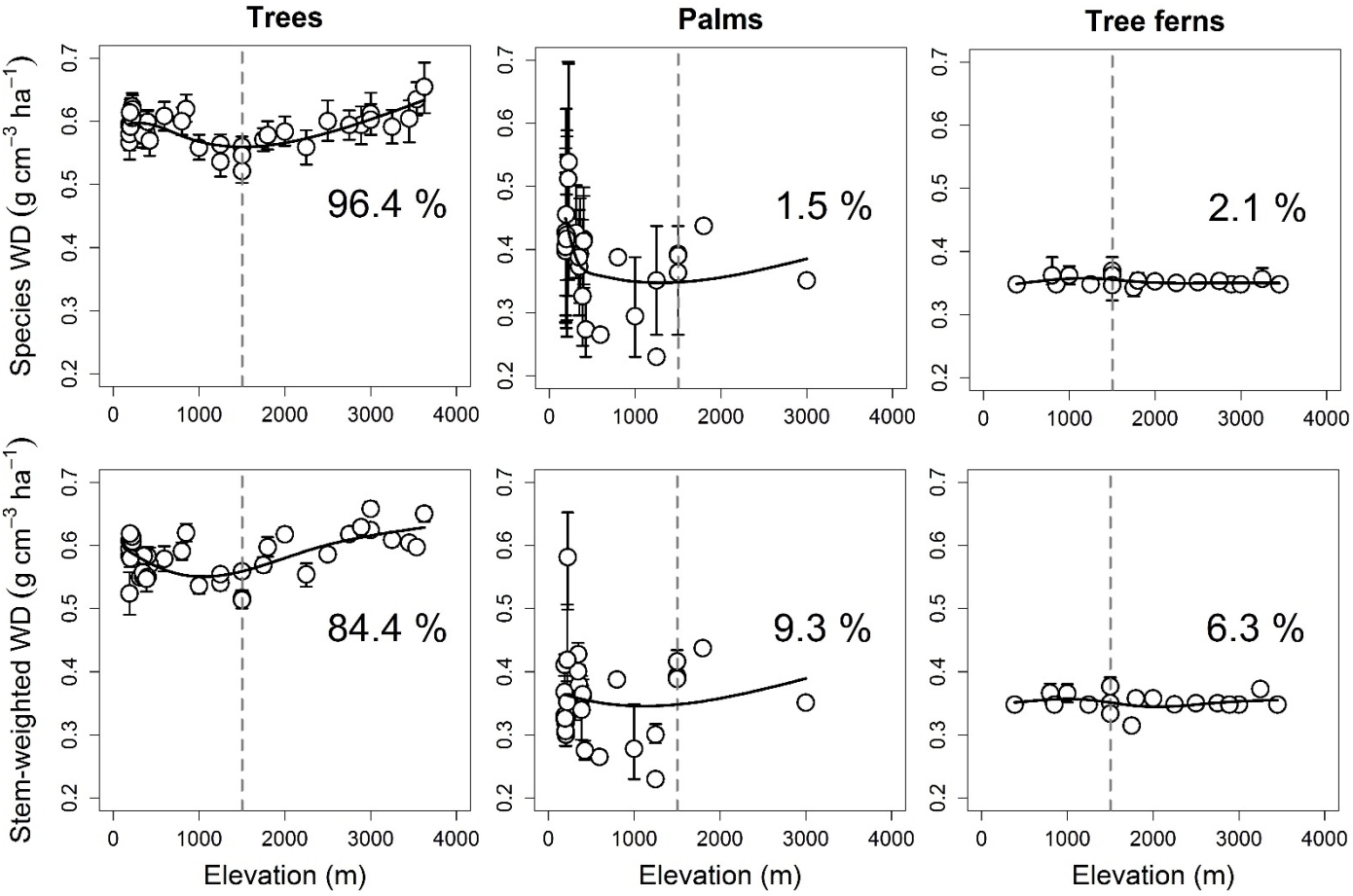

910

911

912

913

914 **Fig. S5.** Plot-level mean wood density variation for trees, palms, and tree ferns along the Andes-
915 to-Amazon elevational gradient. The upper panels represent the species' mean wood density, and
916 the lower panels represent the stem-weighted wood density. Dashed vertical lines indicate the
917 cloud base across the gradient. Percentages indicate the contribution of each life form to the
918 overall wood density for species and Stem-weighted WD.

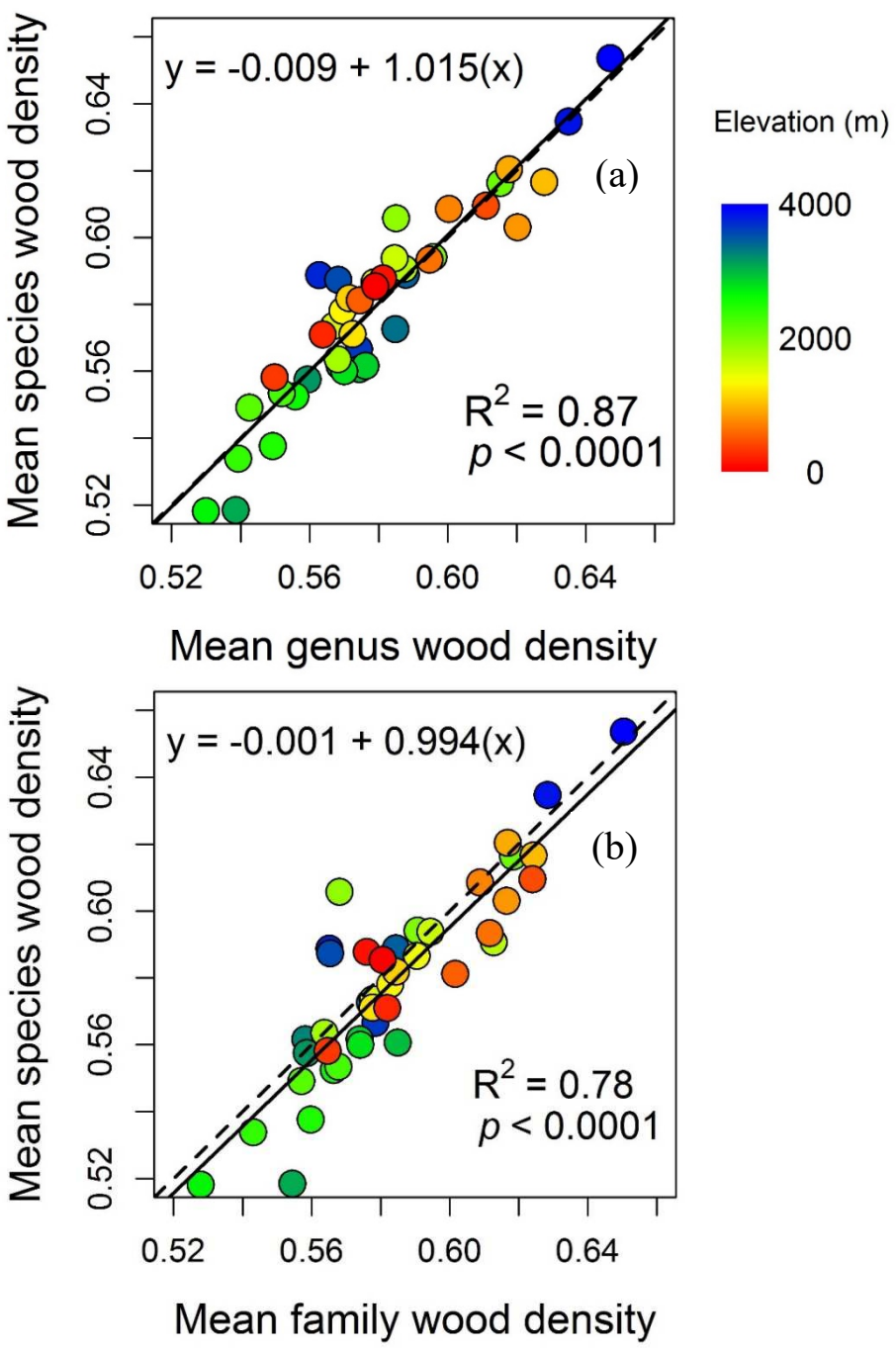

Fig. S6. Mean plot-level wood density for (a) genus and (b) family basis in function of species wood density. Solid lines represent best-fit linear regressions, dashed lines represent the 1:1 relationship. Color ramp corresponds to plot elevations from the highest (blue) to the lowest (red) forest plots. The legend corresponds to the same forest plot colors for panels (a) and (b).